PLOS | ONE

RESEARCH ARTICLE

Pattern Selection in Network of Coupled Multi-Scroll Attractors

Fan Li[1,2], **Jun Ma**[3]*

1 Wuhan Institute of Physics and Mathematics, Chinese Academy of Sciences, Wuhan, 430071, China, **2** University of Chinese Academy of Sciences, Beijing, 100049, China, **3** Department of Physics, Lanzhou University of Technology, Lanzhou, 730050, China

* hyperchaos@163.com

Citation: Li F, Ma J (2016) Pattern Selection in Network of Coupled Multi-Scroll Attractors. PLoS ONE 11(4): e0154282. doi:10.1371/journal.pone.0154282

Editor: Irene Sendiña-Nadal, Universidad Rey Juan Carlos, SPAIN

Received: February 12, 2016

Accepted: April 11, 2016

Published: April 27, 2016

Data Availability Statement: All relevant data are within the paper and its Supporting Information files. For more detailed information please ask help from Dr. Li F at lifan0226@126.com.

Funding: This project is partially supported by the National Natural Science Foundation of China under Grant Nos. 11265008, 11365014, and 61164006. The funders had no role in study design, data collection and analysis, decision to publish, or preparation of the manuscript.

Competing Interests: The authors have declared that no competing interests exist.

Abstract

Multi-scroll chaotic attractor makes the oscillator become more complex in dynamic behaviors. The collective behaviors of coupled oscillators with multi-scroll attractors are investigated in the regular network in two-dimensional array, which the local kinetics is described by an improved Chua circuit. A feasible scheme of negative feedback with diversity is imposed on the network to stabilize the spatial patterns. Firstly, the Chua circuit is improved by replacing the nonlinear term with Sine function to generate infinite aquariums so that multi-scroll chaotic attractors could be generated under appropriate parameters, which could be detected by calculating the Lyapunov exponent in the parameter region. Furthermore, negative feedback with different gains (D_1, D_2) is imposed on the local square center area A_2 and outer area A_1 of the network, it is found that spiral wave, target wave could be developed in the network under appropriate feedback gain with diversity and size of controlled area. Particularly, homogeneous state could be reached after synchronization by selecting appropriate feedback gain and controlled size in the network. Finally, the distribution for statistical factors of synchronization is calculated in the two-parameter space to understand the transition of pattern region. It is found that developed spiral waves, target waves often are associated with smaller factor of synchronization. These results show that emergence of sustained spiral wave and continuous target wave could be effective for further suppression of spatiotemporal chaos in network by generating stable pacemaker completely.

Introduction

Patterns formation and control in spatiotemporal systems have been extensively investigated in the last decades. It is confirmed that various patterns could be observed in physical, chemical, and biological systems, and it is believed that numerical investigation could be feasible to explore some main properties of spatial patterns in dynamical systems. Spiral wave is a class of spatiotemporal pattern, it could be found in the oscillatory and excitable media, such as cardiac tissue [1] and CO oxidation on Pt(110) surface [2]. It has been confirmed that there are involvements of spiral waves in both atrial and ventricular [3–5]. The sudden cardiac death

resulting from ventricular fibrillation is due to the fragment or breakup of the spiral wave and the potential mechanism for breakup of spiral wave has been detected [6]. Target wave could be generated by the concentric waves that are periodically emitted from a small central region [7], and is regarded as the generic for dissipative systems far from equilibrium. Transition of spiral wave, target wave and broken patterns can be induced in possible schemes [8–10].

In general way, the reaction-diffusion system [11–16], coupled oscillators with array type [17], network of coupled neurons (Hodgkin-Huxley, Hindmarch-Rose, Morris-Lecar) [18–24] are suitable for generating spiral wave, target wave and even spatiotemporal chaos in numerical studies. For example, He et al. [17] reported that the spiral waves could be formed in an inhomogeneous excitable medium with small-world connections under an optimal fraction of random connections. Wu et al. [18] gave detailed discussion about potential mechanism for pattern selection in neuronal network. Perc [19] discussed the effect of noise on the pattern formation in the small-world network. Ma et al. [20] detected the stability and transition of spiral wave of network by changing the probability of long range connection. Qin et al. [21] reported that target wave and spiral wave could be induced with feedback forcing current on the membrane potential with different certain time-delays and gains. Roxin et al. investigated the self-sustained wave formation of coupled neurons connected with small-world type. Wang et al. [23] reported that the time delay enhance the coherence of spiral waves for Hodgkin-Huxley neuronal with noise. Interestingly, spirals distribution was found in disinhibited mammalian neocortex [25–27] for experimental evidences, similar to the target wave, these ordered waves can regulate the collective behaviors of network like a continuous pacemaker. In fact, the formation and development of spatial regularity could be associated with the self-organization and competition among complex spatiotemporal system. In dynamical view, the developed states of spatiotemporal system and network depend on the initial states, topology connection (regular connection or small-world connection type), and bifurcation parameters. Li et al. [26] reported that the target wave and spiral wave could be induced by a localized inhomogeneity on spatiotemporal chaotic state, suggested that mechanisms underlying the inhomogeneity sustained coherent wave patterns seem quite different for oscillatory and stationary inhomogeneities. For example, defects block [28] can induce formation of spirals in network, external forcing with diversity [29], inhomogeneity in medium [30], noise[31–34], electric field depolarization [35–38] can greatly change the dynamics of spiral wave and target waves in the spatiotemporal system. Gosak et al. [31] studied the spatial dynamics of excitable media under the subthreshold periodic pacemaker activity and internal noise. Hou et al [32] investigated the spiral wave induced by the temporal noise, the spatial disorder and spatiotemporal fluctuation on the formation of spiral waves are discussed in detail. Tang et al. [33] confirmed that optimal noise could be useful to induce spirals in neuronal network under coherence resonance. Chen et al.[37] investigated the breakup of spiral wave and consequent patterns under the strong polarized advective field, the results shown that the symmetry and chirality of the applied external field are important to form the new-formed patterns. Jiang et al.[38] investigated the emergence of target waves in a cyclic predator-prey model, the results shown that the pattern formation resulting from the interplay between local and global dynamics in systems governed by cyclically competing species. That is to say, pattern formation is often associated with the collective behaviors of coupled oscillators or nodes. For a review about collective behaviors of coupled neurons and pattern transition, please refer to Refs.[39,40].

In the case of collective behaviors of coupled oscillators and network, the local kinetics of node is often supposed under periodical rhythm or chaotic property. Indeed, oscillator with multi-scroll attractors could show more complex dynamical behavior and the collective behavior of these coupled attractors could become more interesting. In dynamical control, many effective schemes [41–46] are used to generate multi-scroll attractors and wings in low-

dimensional chaotic oscillators by replacing the nonlinear term with appropriate piecewise-linear functions or jerk function. In a feasible way, a type of Sine function is used to replace the nonlinear term in the Chua circuit so that infinite scroll attractors could be induced [46], and extensive results are reproduced in PSpice [47]. In this paper, we will study the pattern formation of coupled Chua circuits with infinite scrolls attractors, which are generalized by replacing the nonlinear term in classic Chua circuit [46] with a type of Sine function, so infinite equilibrium points are generated. Furthermore, a method of gradient negative feedback (feedback coefficient with diversity) is presented to generate certain ordered patterns. The network is divided into two regions: local square central region($A_2 = n \times n$) and the rest part of the network (A_1), and then the different negative feedback coefficients are imposed on the two parts respectively. It is found that different kinds of ordered patterns (spiral wave, target wave and breakup pattern) could be developed under different gradient feedback coefficients and appropriate sizes of feedback region (A_2).

Models, Schemes and Results

Multi-scrolls attractors of Chua circuit

The generalized Chua circuit [45, 46] with nonlinear function is described as follows

$$\begin{cases} \dot{x} = \alpha(y - f(x)) \\ \dot{y} = x - y + z \\ \dot{z} = -\beta y \end{cases} \tag{1}$$

The parameter $\alpha = 10.814$, $\beta = 14$, as reported in Ref.[45,46], the Josephson junction is effective to generate multi-scrolls attractor in the Jerk and Chua circuits driven by a Sine function. The underlying mechanism is considered as that the nonlinear system has a group of equilibrium points if the nonlinear term is described by a type of Sine function. As a result, we can replace the nonlinear term in Eq 1 with a similar Sine function, and it reads

$$f(x) = a\sin(2\pi bx) \tag{2}$$

where a, b are parameters in Chua circuit, and then a group of equilibrium points are approached as $(n/2b, 0, -n/2b)$, $n = 0, 1, 2, 3, \ldots$. The largest Lyapunov exponent spectrum is calculated to find the parameter region for chaos emergence. As a result, the distribution in Fig 1 for the largest Lyapunov exponent spectrum of Eq 1 is plotted in the two-parameter space of a and b. The nonlinear system of Eq 1 is in chaotic state, when the largest Lyapunov exponent is positive.

It is found in Fig 1 that the appropriate parameter could induce the chaotic state in Eq 1. Furthermore, the phase portraits are shown in Fig 2 to discern the portrait of multi-scroll attractors. It is confirmed that the number of scrolls increases with calculating time because more equilibriums are generated driven by Sine function. Extensive results confirmed that Hamilton energy is decreased with increasing the number of attractors [48] in chaotic oscillator.

The results in Fig 2 indicated that the number of scrolls depends on the calculating time, and longer transient period is helpful to generate more scroll attractors in this chaotic oscillator. In fact, the collective behaviors of coupled multi-scroll attractors could become more complex. For simplicity, 200×200 Chua circuits with infinite-scrolls attractor are distributed in a two- dimensional lattice network with no-flux boundary condition being considered.

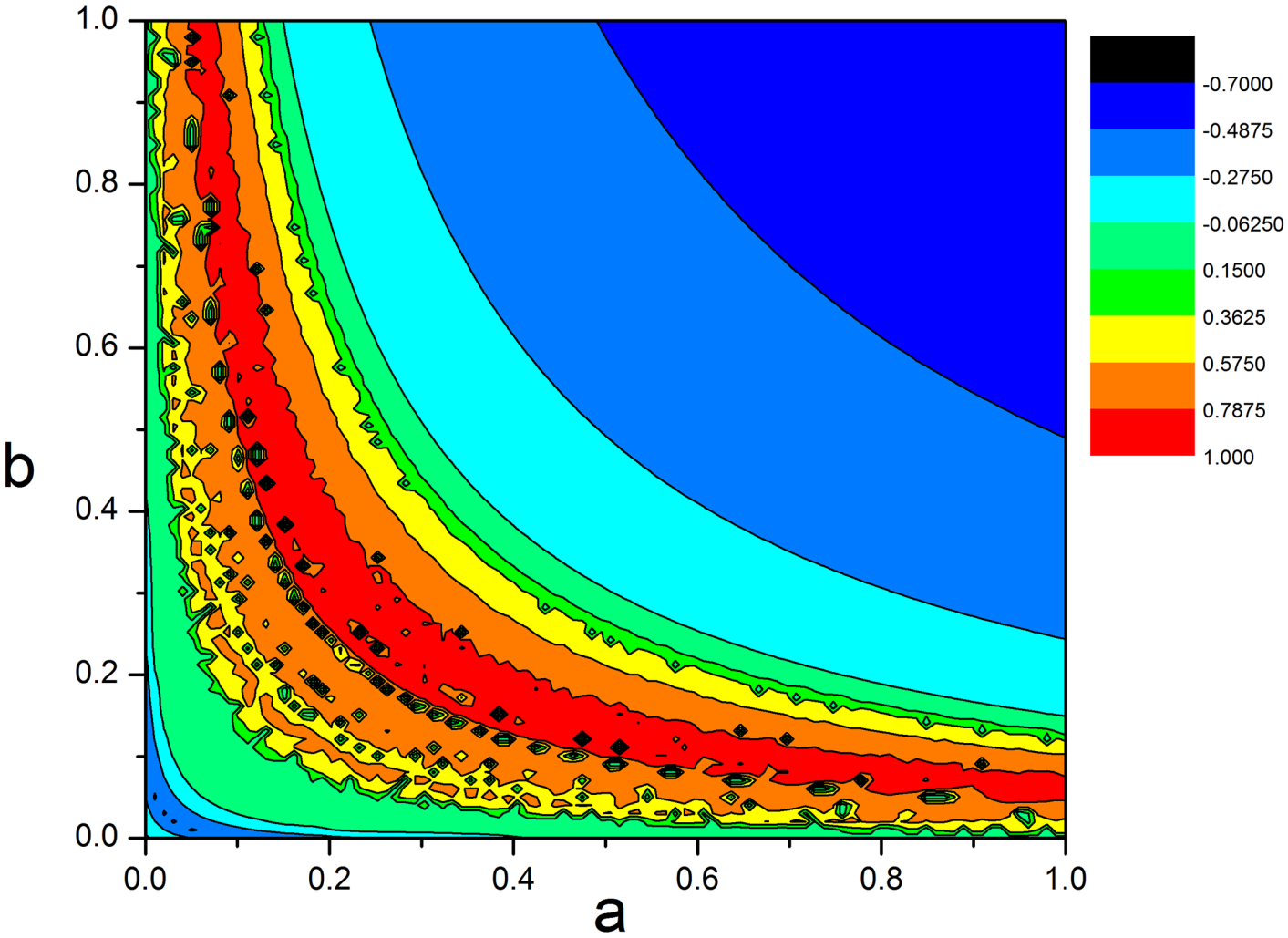

Fig 1. Distribution for the largest Lyapunov exponent for Eq 1 in the two-parameter space. The snapshots are plotted in color scale at $\alpha = 10.814$, $\beta = 14$.

doi:10.1371/journal.pone.0154282.g001

The network of Chua circuits with infinite-scrolls attractor

The network of the coupled Chua circuits with infinite-scrolls attractor with nearest-neighbor coupling is described by

$$\begin{cases} \dot{x}_{ij} = \alpha(y_{ij} - a\sin(2\pi b x_{ij})) + k_1(x_{ij+1} + x_{ij-1} + x_{i+1j} + x_{i-1j} - 4x_{ij}) \\ \dot{y}_{ij} = x_{ij} - y_{ij} + z_{ij} + k_2(y_{ij+1} + y_{ij-1} + y_{i+1j} + y_{i-1j} - 4y_{ij}) \\ \dot{z}_{ij} = -\beta y_{ij} + k_3(z_{ij+1} + z_{ij-1} + z_{i+1j} + z_{i-1j} - 4z_{ij}) \end{cases} \quad (3)$$

where $\alpha = 10.814$, $\beta = 14$, $a = 0.2$, $b = 0.15$, parameter k_1, k_2, k_3 is couple intensity, and all the Chua circuits in the network are identical. Preliminary numerical simulation found that regular pattern can't be formed with single channel coupling ($k_1 \neq 0$, $k_2 = 0$, $k_3 = 0$) and two-channel coupling ($k_1 \neq 0$, $k_2 \neq 0$, $k_3 = 0$), but three-channel coupling ($k_1 \neq 0$, $k_2 \neq 0$, $k_3 \neq 0$) is helpful to induce spatiotemporal patterns. That is to say, one-channel or two-channel coupling

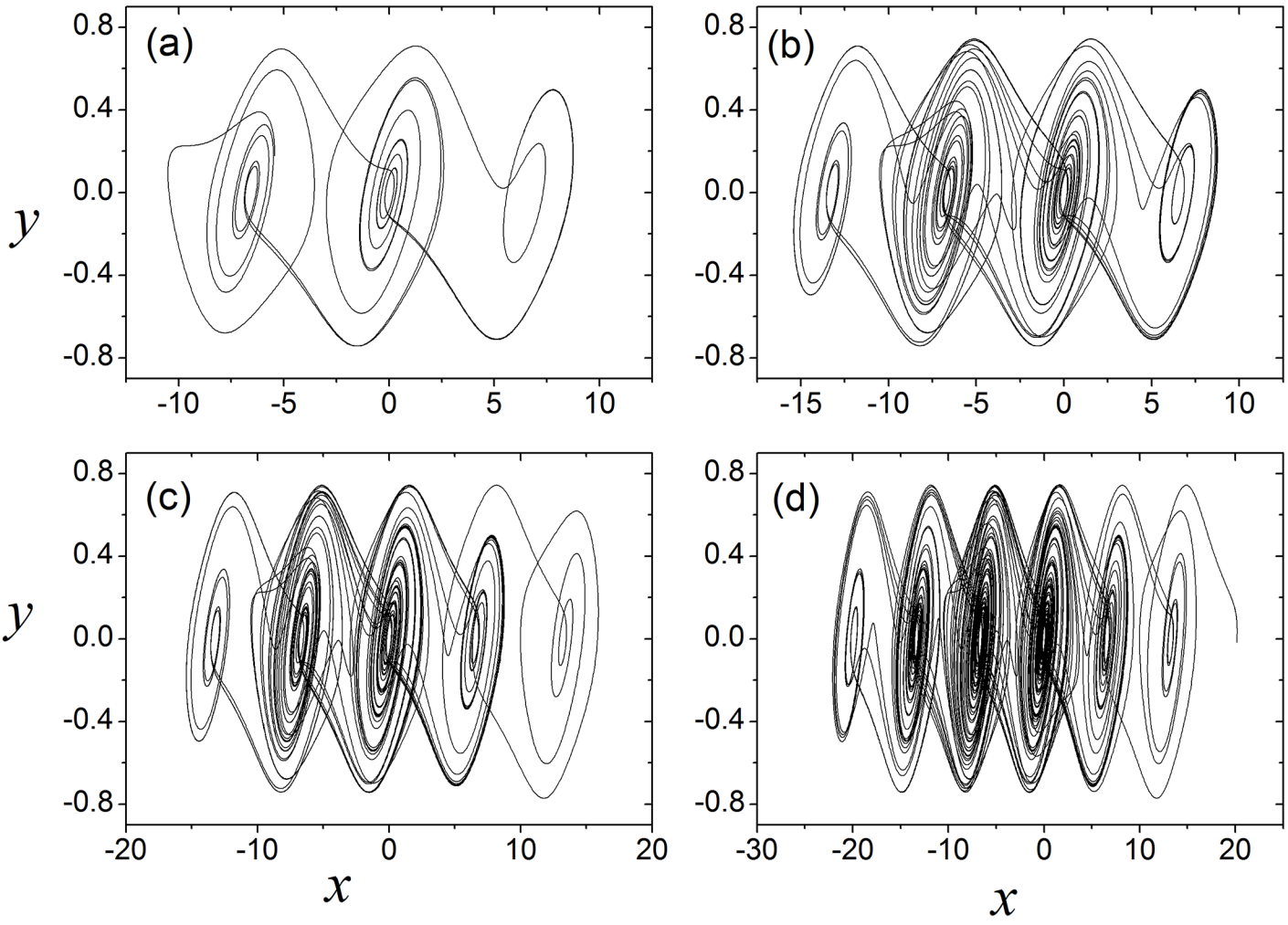

Fig 2. Multi-scrolls attractors are generated within different simulation time. For (**a**) $t = 50$ time units, for (**b**) = 200 time units, for (c) $t = 300$ time units, for (**d**) $t = 500$ time units, $\alpha = 10.814$, $\beta = 14$, $a = 0.2$, $b = 0.15$.

doi:10.1371/journal.pone.0154282.g002

can't support regular spatial patterns but induce broken segments or spatiotemporal chaos in the network. To investigate the transition of spatial patterns, three-channel coupling is applied to induce regular patterns in the network. However, the developed patterns induced by three-channel coupling is not stable, it is changed with increasing time, and stable ordered patterns could not be induced with special initial values, the results are plotted in Fig 3.

The results in Fig 3 confirmed that the developed spatial patterns keep unstable and multi-stability states coexist with the increasing of number of scroll-attractors. Therefore, it is important to find feasible ways to stabilize these unstable patterns. Some general methods are checked to produce ordered pattern in the network described by Eq 3, such as: (i)Special initial values, (ii)Inhomogeneity medium, (iii)Periodic external forcing signal on the border or central region of the networks, (iv) Phase space compression. Unfortunately, extensive numerical results show that the stable ordered pattern can't be developed under these conditions. Fortunately, gradient negative feedback is presented to induce the ordered pattern, and the results found the emergence of spiral wave, target wave and breakup pattern under appropriate conditions.

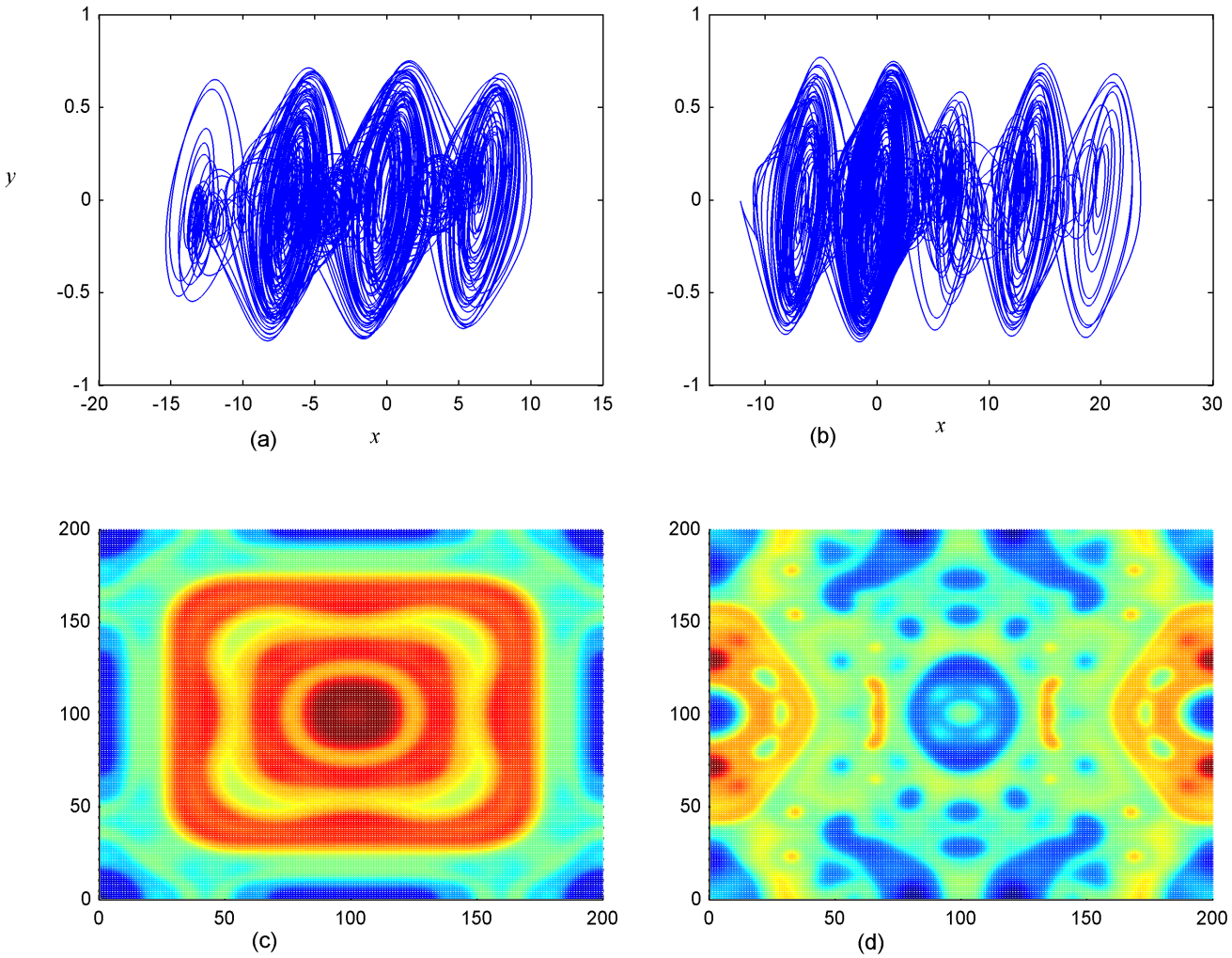

Fig 3. Attractors and spatial patterns. (a-b) the 4-scroll attractors for node (5,5) and 5-scroll attractor for node(50,50), respectively; The developed spatial pattern, for $t = 40$ **(c)**, $t = 1000$ **(d)** time units. The coupling intensity is selected as $k_1 = k_2 = k_3 = 5.5$.

doi:10.1371/journal.pone.0154282.g003

Gradient Negative Feedback for the network

The method of gradient negative feedback is realized by dividing the network into two parts: central square area($A_2 = n \times n$) (6×6, 11×11, 16×16, . . .,) and outer area of the network(A_1), and then different values of negative coupling coefficients(D_1 and D_2) are imposed on the two areas (A_1 and A_2) of the network, respectively. For showing the method clearly, the schematic diagram is shown in Fig 4.

For simplicity, makes $k_1 = k_2 = k_3 = k$, and the network driven by gradient feedback is described by

$$\begin{cases} \dot{x}_{ij} = \alpha(y_{ij} - a\sin(2\pi b x_{ij})) + k(x_{ij+1} + x_{ij-1} + x_{i+1j} + x_{i-1j} - 4x_{ij}) - Dx_{ij} \\ \dot{y}_{ij} = x_{ij} - y_{ij} + z_{ij} + k(y_{ij+1} + y_{ij-1} + y_{i+1j} + y_{i-1j} - 4y_{ij}) - Dy_{ij} \\ \dot{z}_{ij} = -\beta y_{ij} + k(z_{ij+1} + z_{ij-1} + z_{i+1j} + z_{i-1j} - 4z_{ij}) - Dz_{ij} \\ D = D_1 \ for\ area\ A_1,\ D = D_2 \ for\ area\ A_2 \end{cases} \quad (4)$$

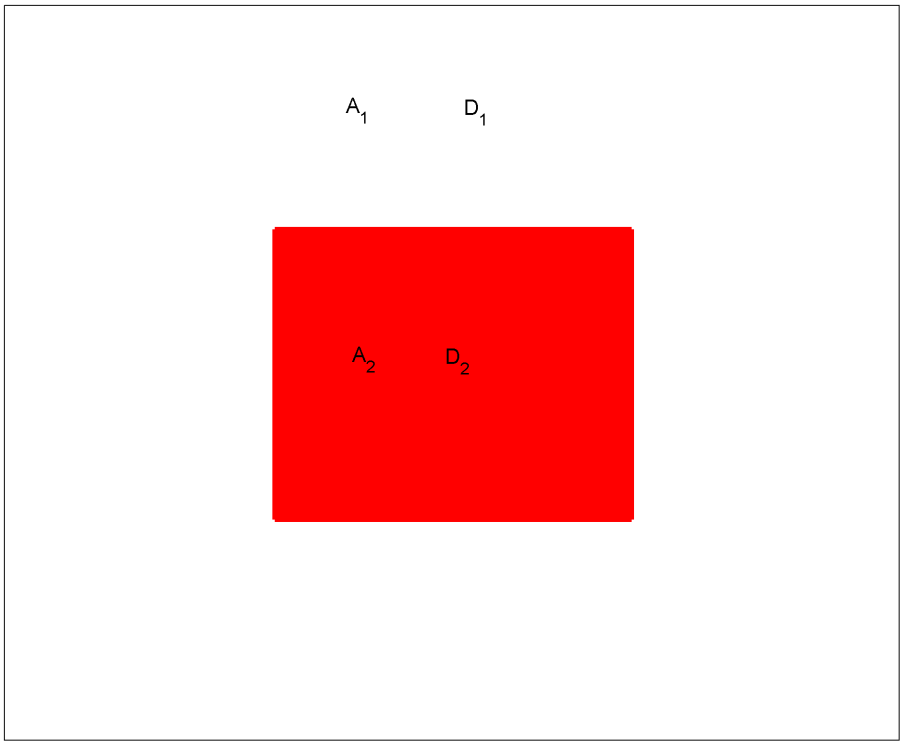

Fig 4. The schematic diagram for gradient negative feedback for network composed of 200×200 identical Chua circuits with infinite-scrolls attractor. A_2 is the size of central square area (red area), and D_2 is the feedback coefficient in the red A_2 area; A_1 is size of the rest area of network (white area), and D_1 is the feedback coefficient in the white A_1 area.

doi:10.1371/journal.pone.0154282.g004

As a result, negative feedback is generated on the network by selecting negative feedback coefficients, D_1 and D_2. Indeed, the effect of negative feedback scheme mainly depends on three effective parameters D_1, D_2 and A_2. In Eq 4, parameters $\alpha = 10.814$, $\beta = 14$, $a = 0.2$, $b = 0.15$, $k = 5.5$, 200 ×200 oscillators are used in the two-dimensional array. It is found that spiral wave, target wave and breakup of patterns cam be observed under appropriate selection for parameters A_2, D_2, D_1, and some results are shown in Fig 5.

The results in Fig 5 confirmed that the developed pattern selection much depends on the parameters in diversity as D_1, D_2, and A_2.

As a result, it is interesting to explore the potential mechanism for this kind of wave formation by checking the time series and dynamical properties of the controlled area, and detailed numerical results could refer to Figs 6 to 15.

Firstly, the effect of factor D_1 on the formation of ordered pattern is investigated. For simplicity, the value of D_1 is selected from 0.1 to 0.5, and the values of D_2, A_2 are fixed certain values. Detailed results are calculated when A_2 area is set as 6×6, 11×11, 16×16, respectively, and the results are plotted in Figs 6–8.

The results in Fig 6 indicated that spiral wave, target wave, homogeneous state could be developed in the network with increasing the value of D_1 from 0.1 to 0.5. Compared the portraits in the first and second panel in Fig 6, it is found that regular spatial distribution could be supported and thus stable spatial patterns could be developed only when the periodicity of the sampled series from area A_2 is approached. Homogeneous state is reached when the center area driven by negative feedback is decreased to stable state. The potential mechanism could be that negative feedback in the center area decrease the chaotic state to periodic or quasi-

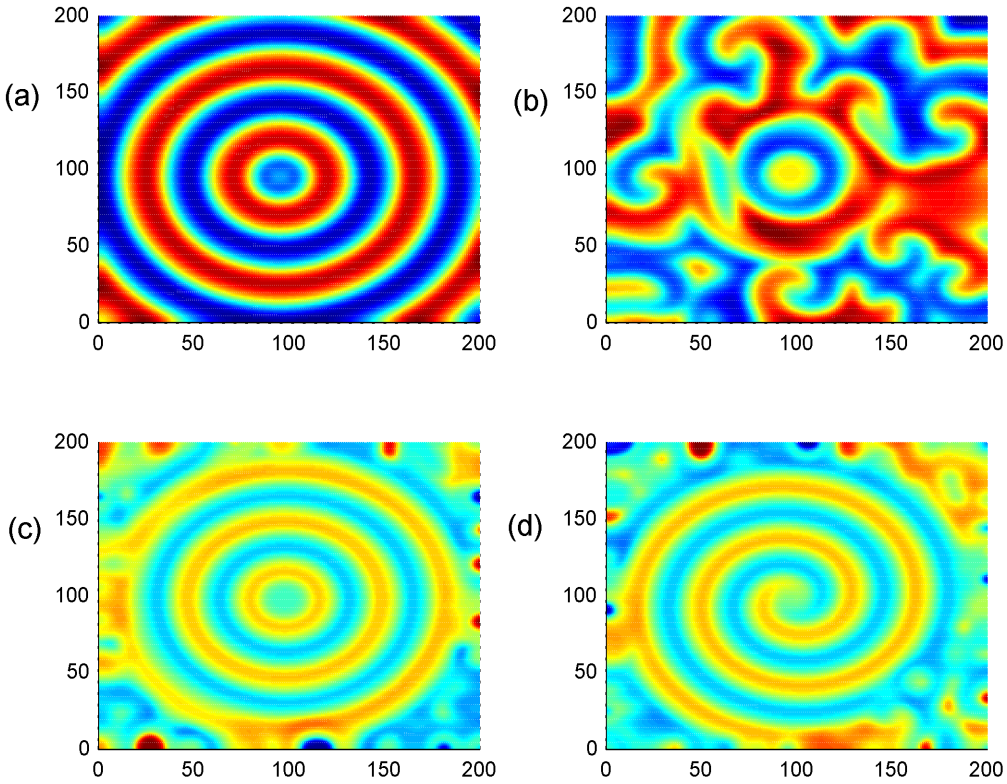

Fig 5. Formation of spatial patterns. (a-d) The developed spatial states with different conditions being used at t = 1000 time units; **(a)** stable target wave at $D_1 = 0.2$, $D_2 = 0.5$, $A_2 = 11\times11(90\leq i, j\leq100)$; **(b)** broken patterns at $D_1 = 0.2$, $D_2 = 0.5$, $A_2 = 15\times15$; **(c)** stable target wave at $D_1 = 0.1$, $D_2 = 0.4$, $A_2 = 15\times15$; **(d)** spiral wave at $D_1 = 0.2$, $D_2 = 0.5$, $A_2 = 16\times16$ $(90\leq i, j\leq105)$.

doi:10.1371/journal.pone.0154282.g005

periodical state even stable state by fixing appropriate feedback coefficients. As a result, a continuous periodic driving emitted from the center areas as a pacemaker thus the collective behaviors of the network could be regulated; finally, stable spatiotemporal patterns could be developed completely. Furthermore, the size of A_2 area is increased to 11×11 and 16×16, and the results are plotted in Figs 7 and 8.

It is found that dynamic properties of sampled series from the same node presented different behaviors when negative feedback on the center area is increased in size, and the collective behaviors and spatial patterns are changed greatly. Surely, negative feedback with stronger intensity just stabilizes the oscillators and the network thus homogeneous states are reached.

By further increasing the center area driven by negative feedback, it is found that stable target wave could be developed under smaller feedback gain in area A_1 and breakup of spatial patterns are also induced by further increasing the feedback gain in center area A_1. Indeed, the sampled series from nodes in area A_1 keep irregular even chaotic and the collective disordered behaviors can't be suppressed even the center control area is enlarged. The results in Figs 6, 7 and 8 confirmed that the developed state and dynamical behaviors of network just depends on the diversity between D_1 and D_2 thus gradient driving could be induced to emit continuous forcing like pacemaker, and the size of center controlled area A_2 also played important role in changing the developed states of the network. In this way, further investigations were carried out thus the effect of feedback gain D_2 and area size could be understood. For simplicity, the feedback gain D_2 in center area A_2 (6×6 nodes) is changed at fixed D_1 = 0.1, 0.2, and the formation of spatial pattern in calculated in Figs 9 and 10. In Figs 11 and 12, different feedback gains

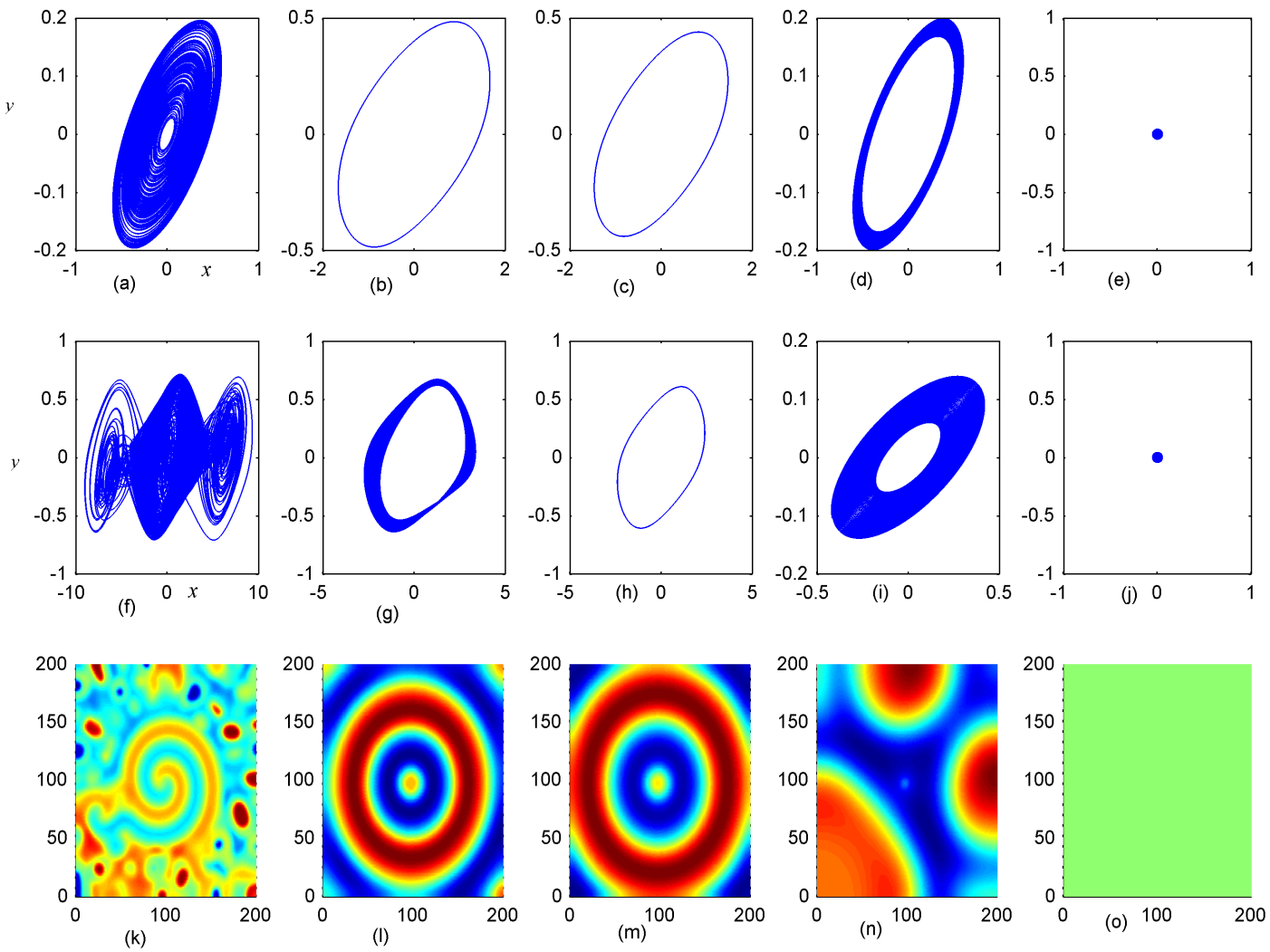

Fig 6. Stabilization of attractors and patterns driven by negative feedback. $A_2 = 6\times6(A_2 = 95\leq i, j\leq 100)$, **(a-e)** the attractors for the node (98, 98) in A_2 area; **(f-j)** the attractors for node (5, 5) in A_1 area; **(k-o)** the snapshots for pattern of the network. **(a, f, k)** $D_1 = 0.1$, $D_2 = 0.5$, $t = 4000$ time units; **(b, g, l)** $D_1 = 0.2$, $D_2 = 0.5$, $t = 1000$; **(c, h, m)** $D_1 = 0.3$, $D_2 = 0.5$, $t = 1000$ time units; **(d, i, n)** $D_1 = 0.4$, $D_2 = 0.5$, $t = 1000$; **(e, j, o)** $D_1 = 0.5$, $D_2 = 0.6$, $t = 1000$ time units.

doi:10.1371/journal.pone.0154282.g006

D_2 are used in the center control area A_2 (11×11 nodes) by fixing the feedback gain $D_1 = 0.1$, 0.2 in the outer area A_1. Furthermore, the center area is increased to A_2 (16×16 nodes) at fixed $D_1 = 0.1$, 0.2 when different feedback gains D_2 is used in the center control area A_2, respectively, and the results are plotted in Figs 13 and 14.

It is confirmed in Fig 9 that spiral waves could be developed in the network for $D_1 = 0.1$ that appropriate diversity in feedback gain is critical to induce continuous travelling waves, which encounter breakup close to the boundary between the two control area of network. Unfortunately, the developed spiral wave just covers certain area of the network and failed to grow up in the network completely. As a result, the phase portraits for the sampled oscillators or nodes often present chaotic attractor instead of periodical periodicity. That is to say, the coexistence between periodic attractors and multi-scroll attractors makes the spiral wave occupy the network in certain size instead of the full area completely.

By further increasing the feedback gain in area A_1 that the diversity in feedback is decreased, it is found in Fig 10 that target wave could be developed because the gradient diversity can't

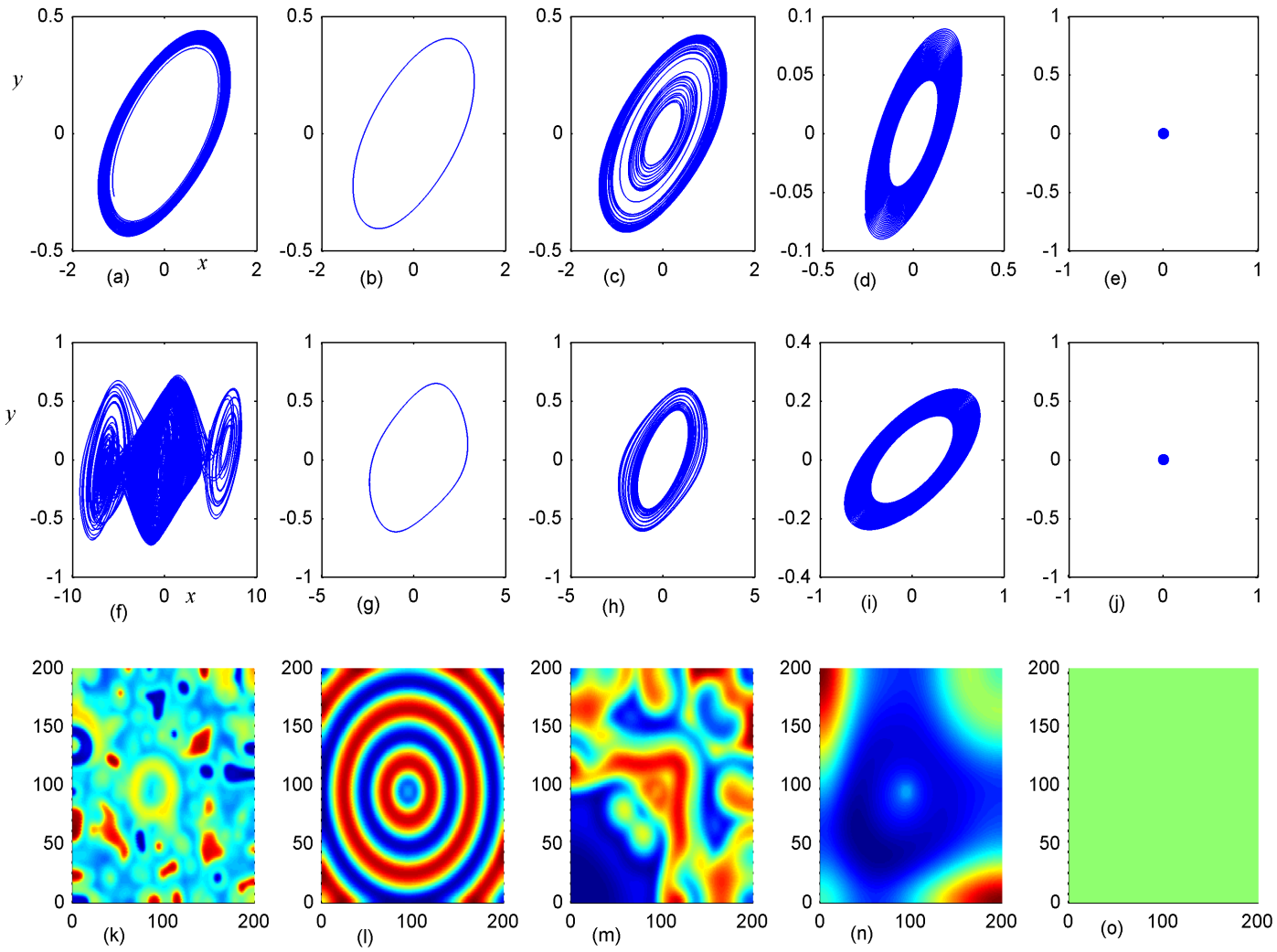

Fig 7. Stabilization of attractors and patterns driven by negative feedback. $A_2 = 11\times11(A_2 = 90\leq i, j\leq100)$, **(a-e)** the attractors for the node (98,98) in A_2 area; **(f-j)** the attractors for node(5,5) in A_1 area; **(k-o)** the snapshot for pattern **(a, f, k)**$D_1 = 0.1$, $D_2 = 0.5$, $t = 4000$; **(b, g, l)** $D_1 = 0.2$, $D_2 = 0.5$, $t = 1000$;**(c, h, m)** $D_1 = 0.3$, $D_2 = 0.5$, $t = 1000$;**(d, i, n)** $D_1 = 0.4$, $D_2 = 0.5$, $t = 1000$; **(e, j, o)** $D_1 = 0.5$, $D_2 = 0.6$, $t = 1000$ time units.

doi:10.1371/journal.pone.0154282.g007

break the target waves emitted from the center area. Particularly, limit circle was observed from the sampled series of monitored nodes, and it indicated distinct periodicity is detected thus continuous target waves are developed in the network. Unfortunately, broken spatial patterns are formed by increasing the center control area A_2 (11×11 nodes), and the results are calculated in Fig 11.

Similar to the results in Fig 9, spiral segments were observed in local area and most of the network was covered by broken segments, and the phase portraits for the sampled nodes presented multi-scroll or chaotic attractors. It indicated that diversity in feedback gain between the two control areas is not effective to induce stable travelling waves. Furthermore, the diversity between feedback gains from the two areas is decreased, and stable target waves could be developed in Fig 12.

The sampled series from the monitored nodes presented distinct periodicity and limit circles are detected when the center controlled area is increased in size under appropriate diversity in

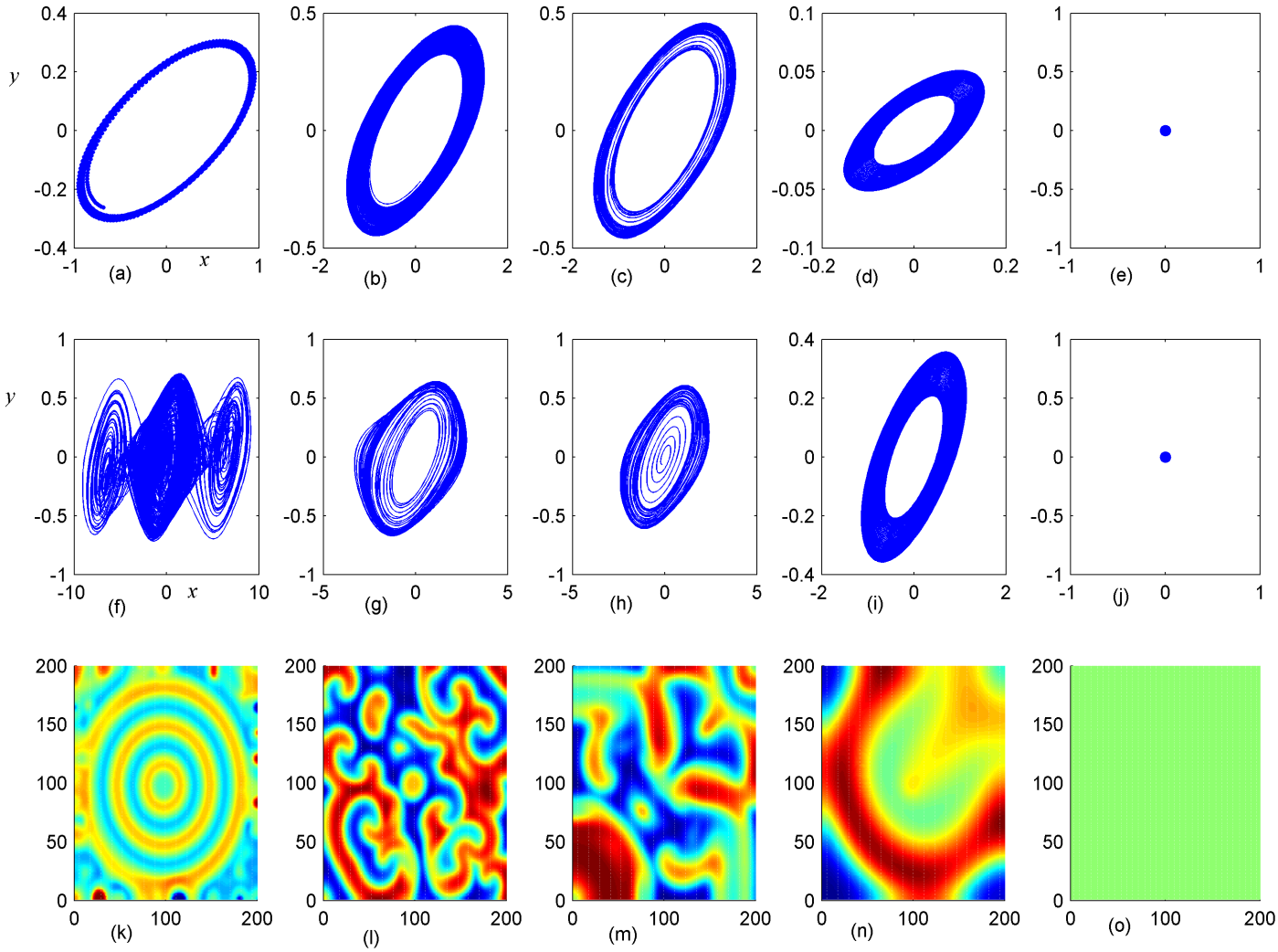

Fig 8. Stabilization of attractors and patterns driven by negative feedback. $A_2 = 16\times16(A_2 = 90\leq i, j\leq105)$, **(a-e)** the attractors for the node (98, 98) in A_2 area; (**f-j)** the attractors for node (5,5) in A_1 area; **(k-o)** the snapshot for pattern of the network. **(a, f, k)** $D_1 = 0.1$, $D_2 = 0.4$, $t = 1000$; **(b, g, l)** $D_1 = 0.2$, $D_2 = 0.4$, $t = 1000$; **(c, h, m)** $D_1 = 0.3$, $D_2 = 0.4$, $t = 1000$; **(d, i, n)** $D_1 = 0.4$, $D_2 = 0.6$, $t = 1000$; **(e, j, o)** $D_1 = 0.5$, $D_2 = 0.6$, $t = 1000$ time units.

doi:10.1371/journal.pone.0154282.g008

feedback gains, and stable target wave began to occupy the network completely. Furthermore, the center controlled area is increased and appropriate feedback gain with diversity is selected to generate perfect spiral wave so that the collective behaviors of network could be regulated by the self-sustained spiral waves, and the results are plotted in Fig 13.

It is interesting to find perfect spiral wave and/or target wave could be developed to occupy the network completely. It was confirmed that appropriate diversity in feedback gain and size of the controlled area are effective to support spiral wave and target wave as well.

Above all, most of cases have been investigated when the feedback gain in the center area A_2 was selected with larger value than the outer area A_1 ($D_2 > D_1$). To further verify the effect of diversity between feedback gain, it is interesting to investigate some cases under $D_2 < D_1$ that similar diversity in feedback gain could be generated, and some results are plotted in Figs 14 and 15 to understand the effect of feedback gain and control area in the formation of spatial patterns.

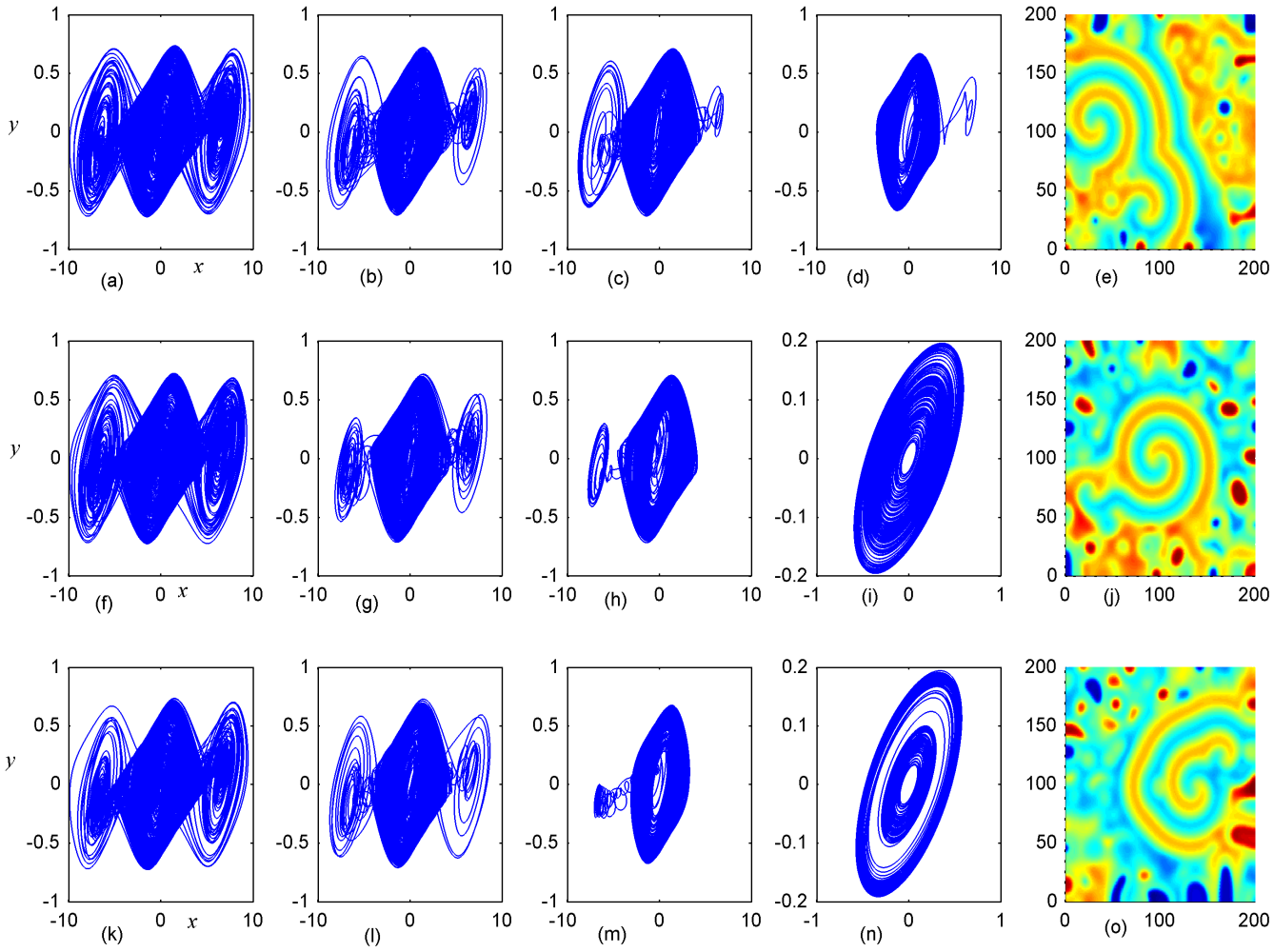

Fig 9. Stabilization of attractors and patterns driven by negative feedback. $D_1 = 0.1$, $A_2 = 6\times6(95\leq i, j\leq100)$, **(a-d)**, **(f-i)**, **(k-n)** the attractors for nodes (5,5), (10,10), (92,92), (98,98) respectively; **(e)**, **(j)**,**(o)** the snapshot for the developed states, respectively; **(a-e)** $D_2 = 0.2$, $t = 4000$; **(f-j)** $D_2 = 0.5$, $t = 4000$; **(k-o)** $D_2 = 2.0$, $t = 4000$ time units.

doi:10.1371/journal.pone.0154282.g009

In the case of $D_1 = 0.1$, the target wave or spiral wave could be induced by setting appropriate value for D_2 and A_2. However, for the case $D_1 = 0.2$, the target wave is only stable with $A_2 \leq 16\times16$ and $D_2 \leq 0.3$, otherwise, breakup of patterns occurs.

Finally, it is interesting to discern some statistical properties of the network during the formation of spatial patterns. Based on the mean filed theory, a statistical factor of synchronization [49] is redefined in the two parameter space [20, 21] to study the robustness of the pattern. The factors of synchronization R is calculated as follows

$$F = \frac{1}{N^2}\sum_{j=1}^{N}\sum_{i=1}^{N} x_{ij} = < x_{ij} >_s \tag{5}$$

$$R = \frac{\langle F^2\rangle - \langle F\rangle^2}{\frac{1}{N^2}\sum_{j=1}^{N}\sum_{i=1}^{N}(\langle x_{ij}^2\rangle - \langle x_{ij}\rangle^2)} \tag{6}$$

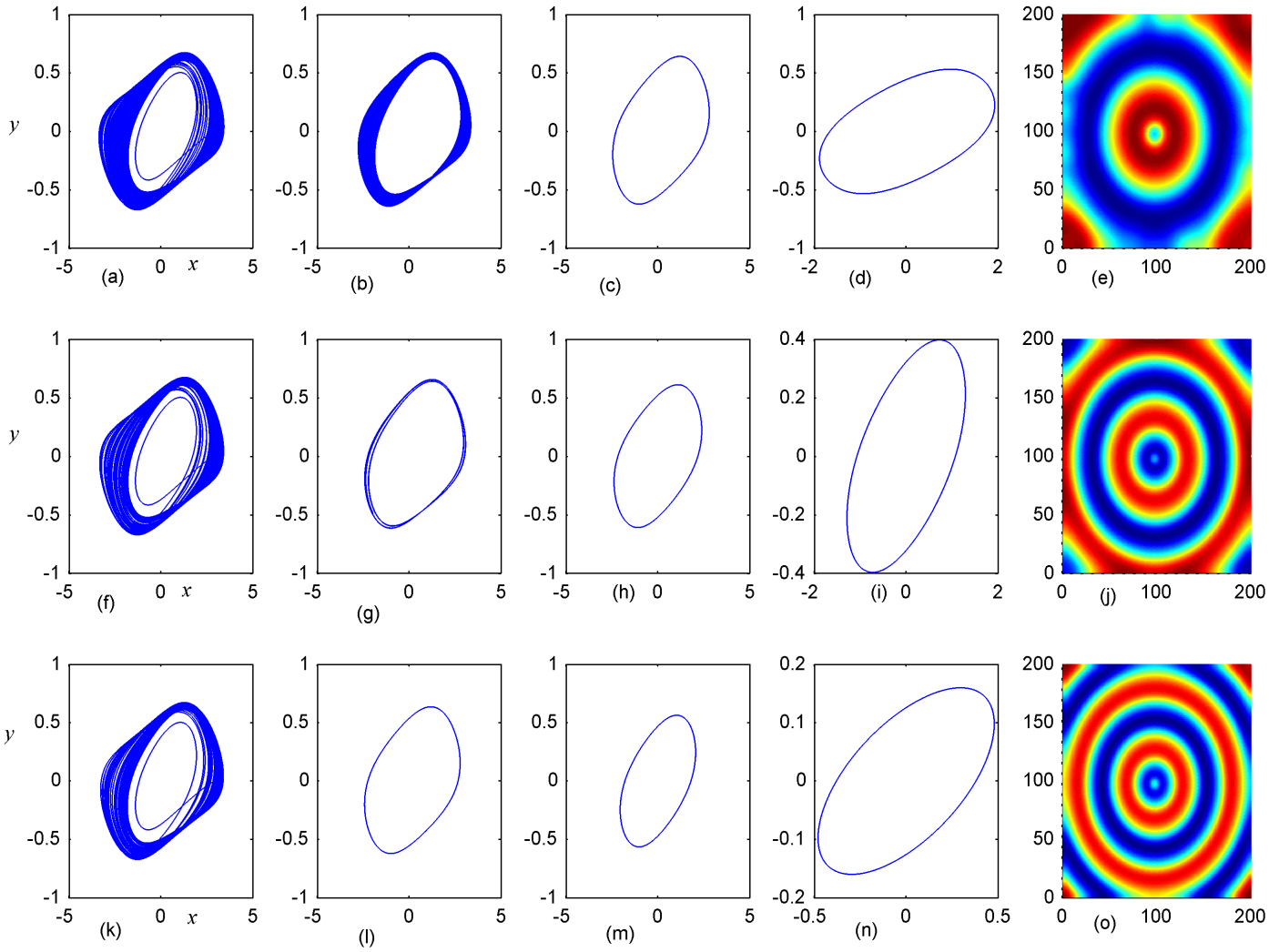

Fig 10. Stabilization of attractors and patterns driven by negative feedback. $D_1 = 0.2$, $A_2 = 6\times6(95\leq i, j\leq100)$, **(a-d),(f-i),(k-n)** the attractors for nodes (5,5), (10,10), (92,92), (98,98) respectively; **(e),(j),(o)** the snapshot for the developed states, respectively; **(a-e)** $D_2 = 0.3$, $t = 1000$; **(f-j)** $D_2 = 0.5$, $t = 1000$; **(k-o)** $D_2 = 2.0$, $t = 1000$ time units.

doi:10.1371/journal.pone.0154282.g010

The variable F is the spatial average value of the detected variables for each node in the network, $<^*>$ indicates the average for calculating time or period. N^2 is the number of nodes in the network, the factor of synchronization R is calculated to detect the transition and stability of developed patterns. It is confirmed that a smaller value R is associated to an ordered state and non-perfect synchronization. Complete perfect synchronization is approached when the factor of synchronization R is much close to 1. As mentioned above, the developed states (spiral wave, target wave, homogeneous state) depend on the selection for feedback gains (D_1, D_2) and the size of center controlled areas A_2. For simplicity, we calculated the distribution of factor of synchronization in the two-parameter space (D_2 *vs.*A_2) at fixed feedback gain $D_1 = 0.1$ and $D_1 = 0.2$, respectively. Furthermore, the pattern region is also calculated in the two-parameter space by detecting the developed states at $t = 1000$ time units. For simplicity, (1) if the pattern could not be induced within 1000 time unites, it is marked as number 0; (2) if target wave is formed within 1000 time unites, it is labeled as 1; if the pattern is breakup, be labeled as 2; (3) if spiral wave is developed, it is labeled as 3, these results are plotted in Fig 15.

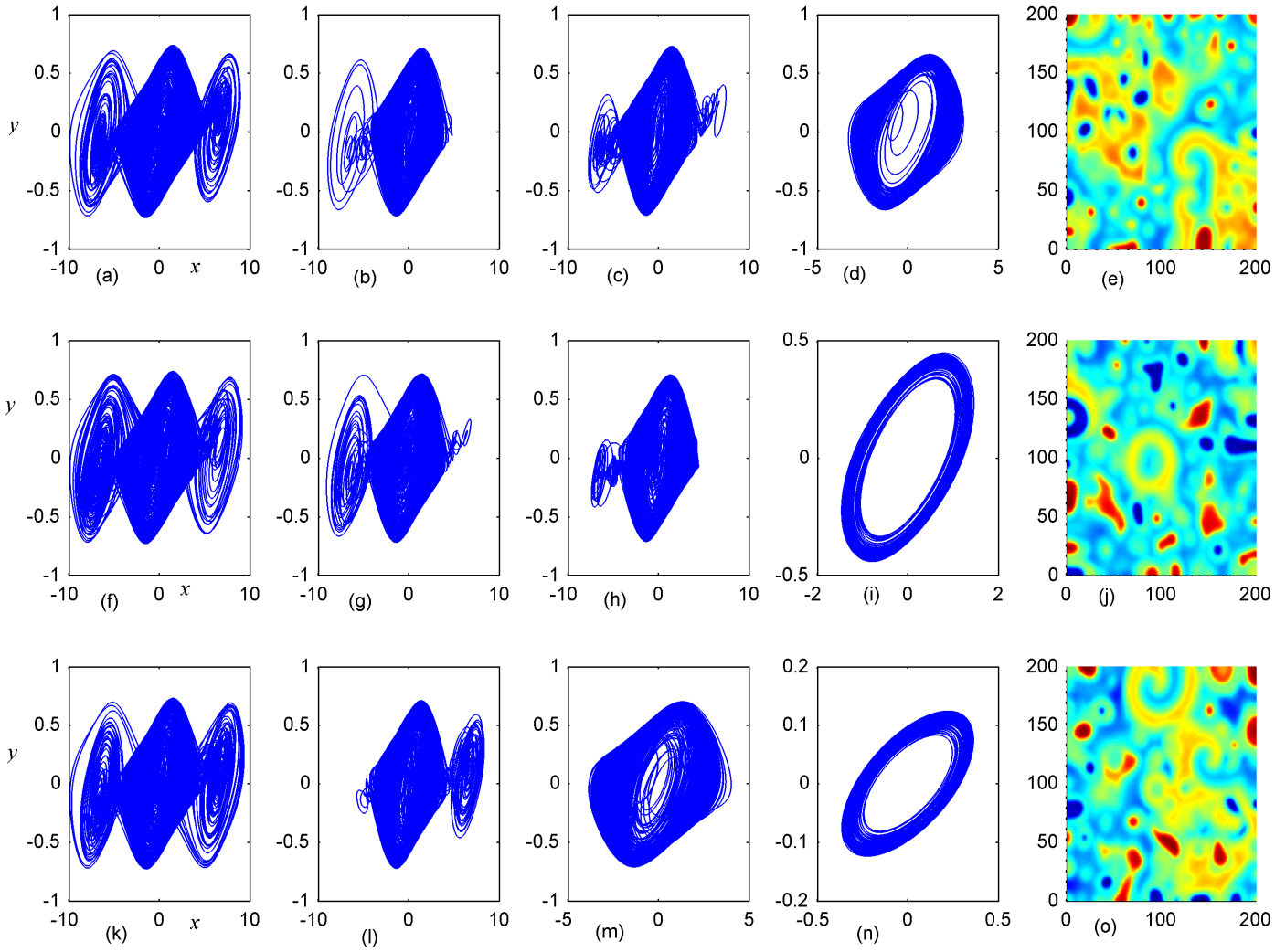

Fig 11. Stabilization of attractors and patterns driven by negative feedback. $D_1 = 0.1$, $A_2 = 11\times11(90\leq i, j\leq100)$, **(a-d),(f-i)**, **(k-n)** the attractors for nodes (5,5), (10,10), (85,85), (98,98), respectively; **(e)**,**(j)**,**(o)** the snapshot for the developed states, respectively; **(a-e)** $D_2 = 0.2$, $t = 4000$; **(f-j)** $D_2 = 0.5$, $t = 4000$; **(k-o)** $D_2 = 2.0$, $t = 4000$ time units.

doi:10.1371/journal.pone.0154282.g011

According to the distribution region in Fig 15, it is confirmed that the developed states and pattern formation are greatly dependent on the selection of feedback gain and the size of the center controlled area as well. Appropriate selection for feedback gain with diversity and size of controlled area can generate appropriate spiral wave, target wave, homogeneous states in the network. The network or the media can show distinct periodicity when spiral wave and/or target wave is developed to occupy the network, and the sampled time series from monitored nodes can present distinct periodicity, and limit circle could also be observed in phase portrait. Surely, network of coupled periodic oscillators even chaotic oscillators can support the emergence of target wave and spiral wave, however, network composed of multi-scroll chaotic oscillators could be passive to support stable ordered waves because its complex dynamical properties in each node that multi-scroll attractors are associated with calculation time. Indeed, spatiotemporal chaos or broken segments in the network could be further suppressed by generating continuous spiral wave or target wave played as a powerful pacemaker.

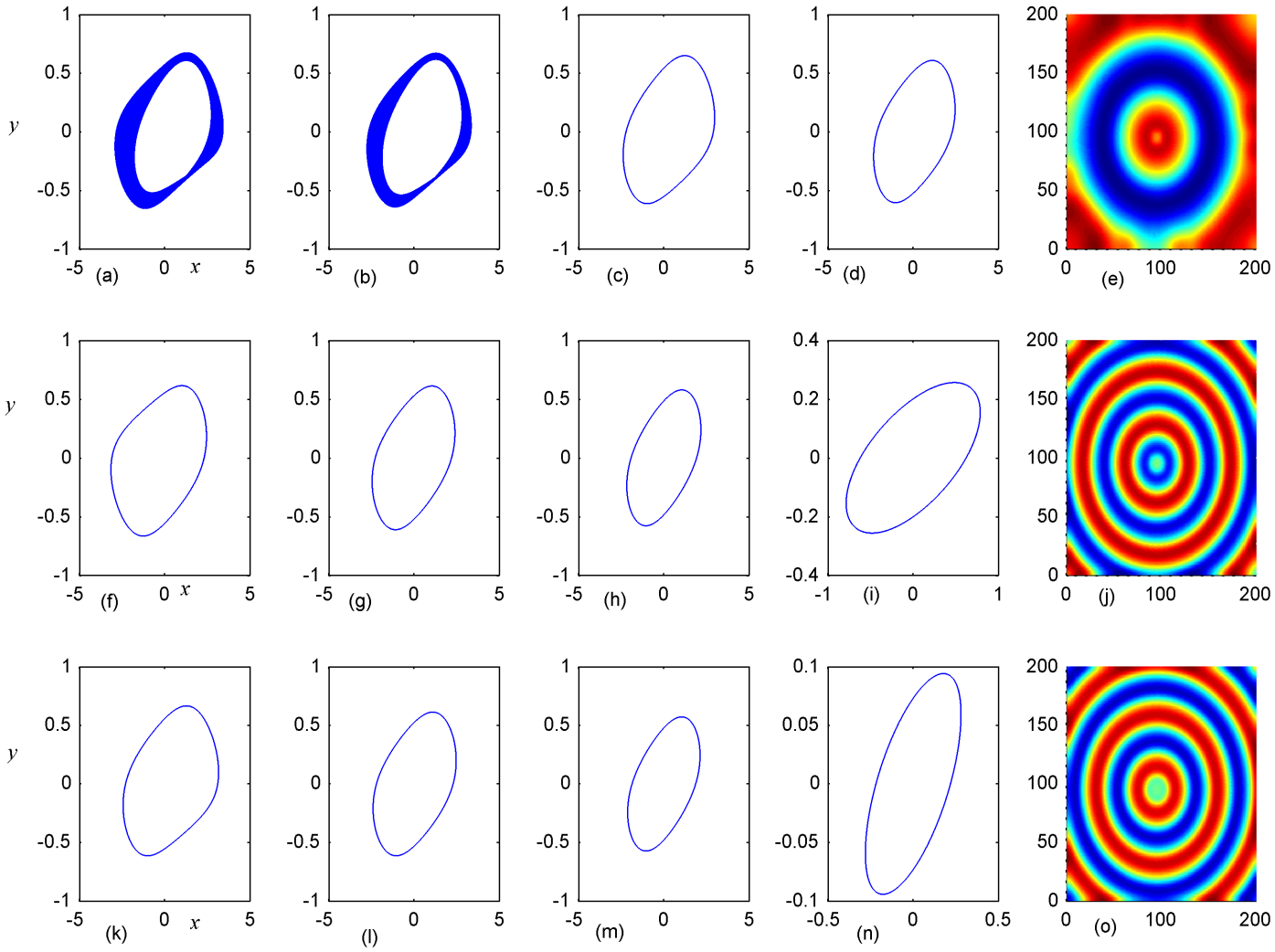

Fig 12. Stabilization of attractors and patterns driven by negative feedback. $D_1 = 0.2$, $A_2 = 11\times11(90\leq i, j\leq100)$, **(a-d),(f-i),(k-n)** the attractors for nodes (5, 5), (10,10), (85, 85), (98, 98), respectively; **(e),(j),(o)** the snapshot for the developed states, respectively; **(a-e)** $D_2 = 0.3$, $t = 1000$; **(f-j)** $D_2 = 0.8$, $t = 1000$; **(k-o)** $D_2 = 2.0$, $t = 1000$ time units.

doi:10.1371/journal.pone.0154282.g012

As mentioned above, statistical factor of synchronization is effective to measure the phase transition and synchronization degree of the collective behaviors of network. Indeed, it is also important to study the synchronization stability of the isolate circuit or node of the network by using the master function approach [50, 51], and the basin area is calculated to discern the dependence of states on selection of initial values, furthermore, bifurcation analysis is also supplied.

The stability of synchronization of the system under multi-variables (channels) coupling

The previous works confirmed that spatial patterns could be selected due to three-channels coupling. To clarify this problem, the dependence of stability of the synchronization on the number of variables coupling is studied by the master stability function. The Eq 3 are written

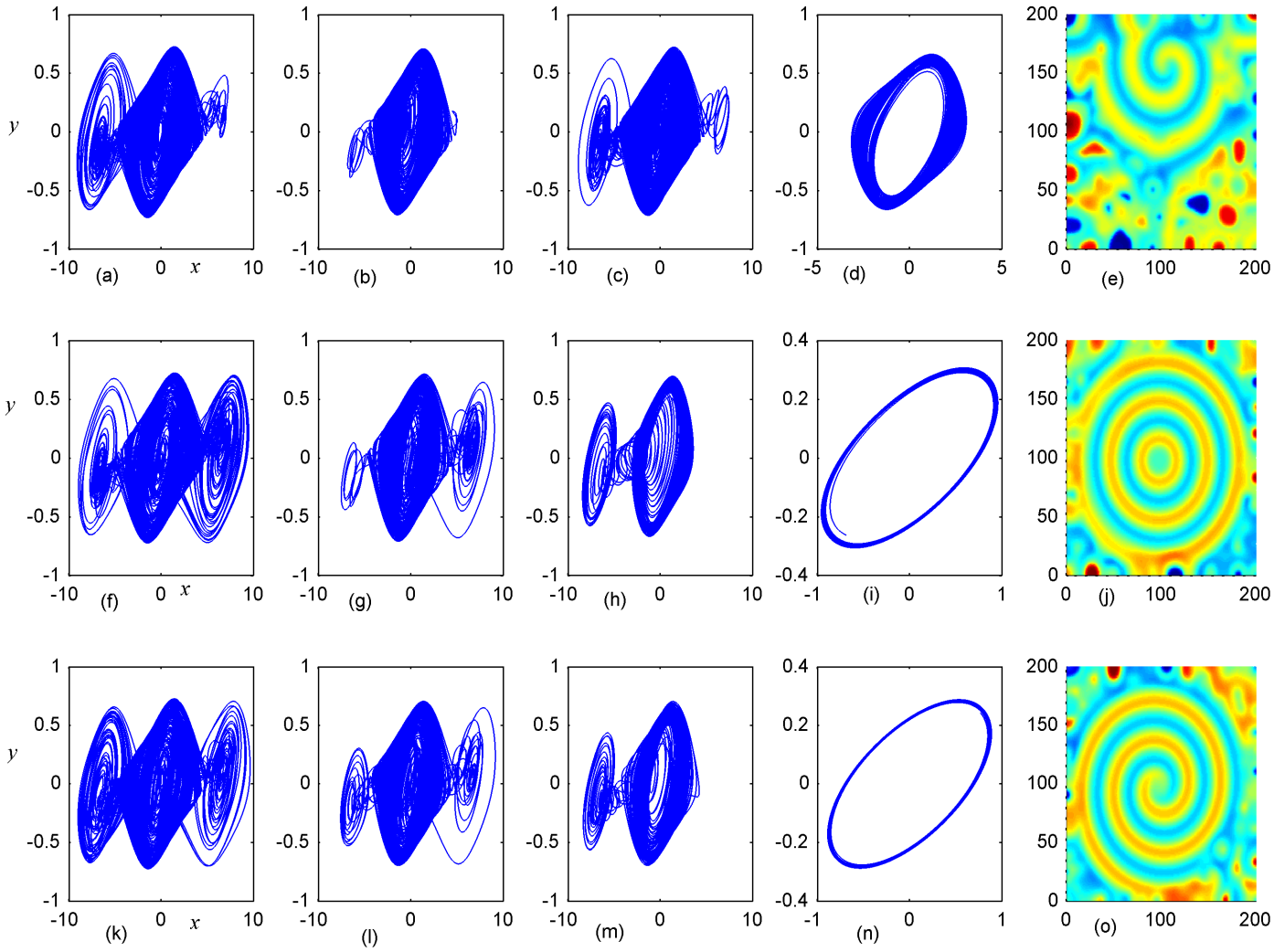

Fig 13. Stabilization of attractors and patterns driven by negative feedback. $D_1 = 0.1$, $A_2 = 16\times16$ ($90\leq i,j\leq105$), **(a-d),(f-i),(k-n)** the attractors for nodes (5,5), (10,10), (85,85), (98,98), respectively; **(e),(j),(o)** the snapshot for the developed states, respectively; **(a-e)** $D_2 = 0.2$, $t = 4000$; **(f-j)** $D_2 = 0.4$, $t = 1000$; **(k-o)** $D_2 = 0.5$, $t = 1000$ time units.

doi:10.1371/journal.pone.0154282.g013

as follows

$$\begin{cases} \dot{x}_i = \alpha(y_i - f(x_i)) + k_1\sum_{j=1}^{N} A_{ij}(x_j - x_i) \\ \dot{y}_i = x_i - y_i + z_i + k_2\sum_{j=1}^{N} A_{ij}(y_j - y_i) \\ \dot{z}_i = -\beta y_i + k_3\sum_{j=1}^{N} A_{ij}(z_j - z_i) \end{cases} \tag{7}$$

where matrix A_{ij} is coupling matrix, according to the master stability function formalism, the

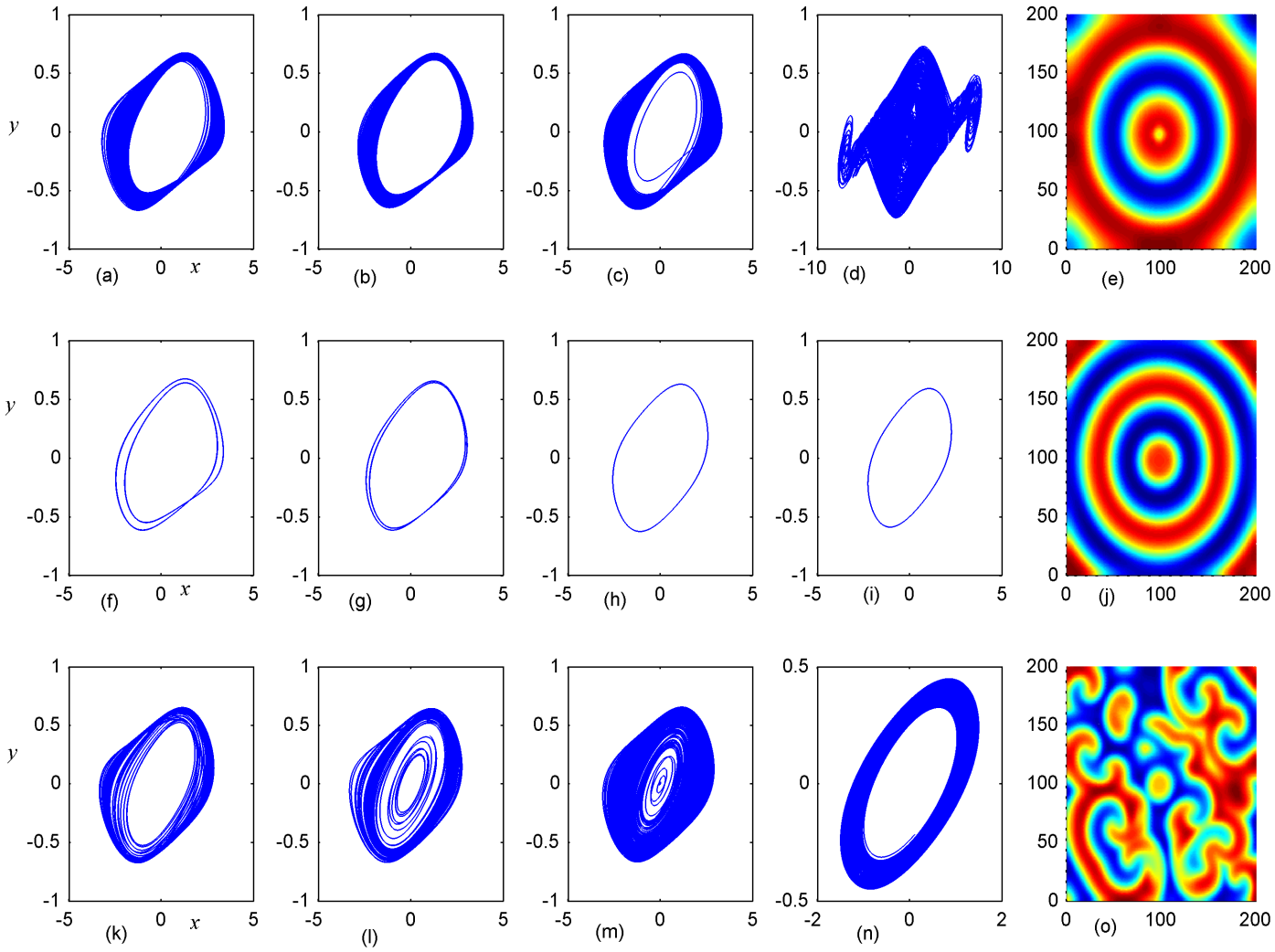

Fig 14. Stabilization of attractors and patterns driven by negative feedback. $D_1 = 0.2$, $A_2 = 16\times16(90\leq i,j\leq105)$, **(a-d), (f-i), (k-n)** the attractors for nodes (5,5), (10,10), (85,85), (98,98), respectively; **(e),(j),(o)** the snapshot for the developed states, respectively; **(a-e)** $D_2 = 0.1$, $t = 1000$; **(f-j)** $D_2 = 0.3$, $t = 1000$; **(k-o)** $D_2 = 0.4$, $t = 1000$ time units.

doi:10.1371/journal.pone.0154282.g014

Eq 7 are described by

$$\begin{aligned}\vec{w}_i &= F(\vec{w}_i) - k_1\sum_{i=1}^{N}L^x{}_{ij}H(x_i) - k_2\sum_{i=1}^{N}L^y{}_{ij}H(y_i) - k_3\sum_{i=1}^{N}L^z{}_{ij}H(z_i)\\ &= F(\vec{w}_i) - k\sum_{i=1}^{N}L_{ij}H(\vec{w}_i)\end{aligned} \tag{8}$$

where $F(\vec{w})$ is dynamical function for the system, Laplacian matrix is selected as the same $L^x_{ij}, L^y_{ij}, L^z_{ij} = L_{ij}$. H($x$), H($y$), H($z$), H($\boldsymbol{w}$) are coupling functions. According to the master stability function presented by Pecora and Carroll [50, 51], the Lyapunov exponents can be determined from a single function that is independent of the network. Therefore, the master

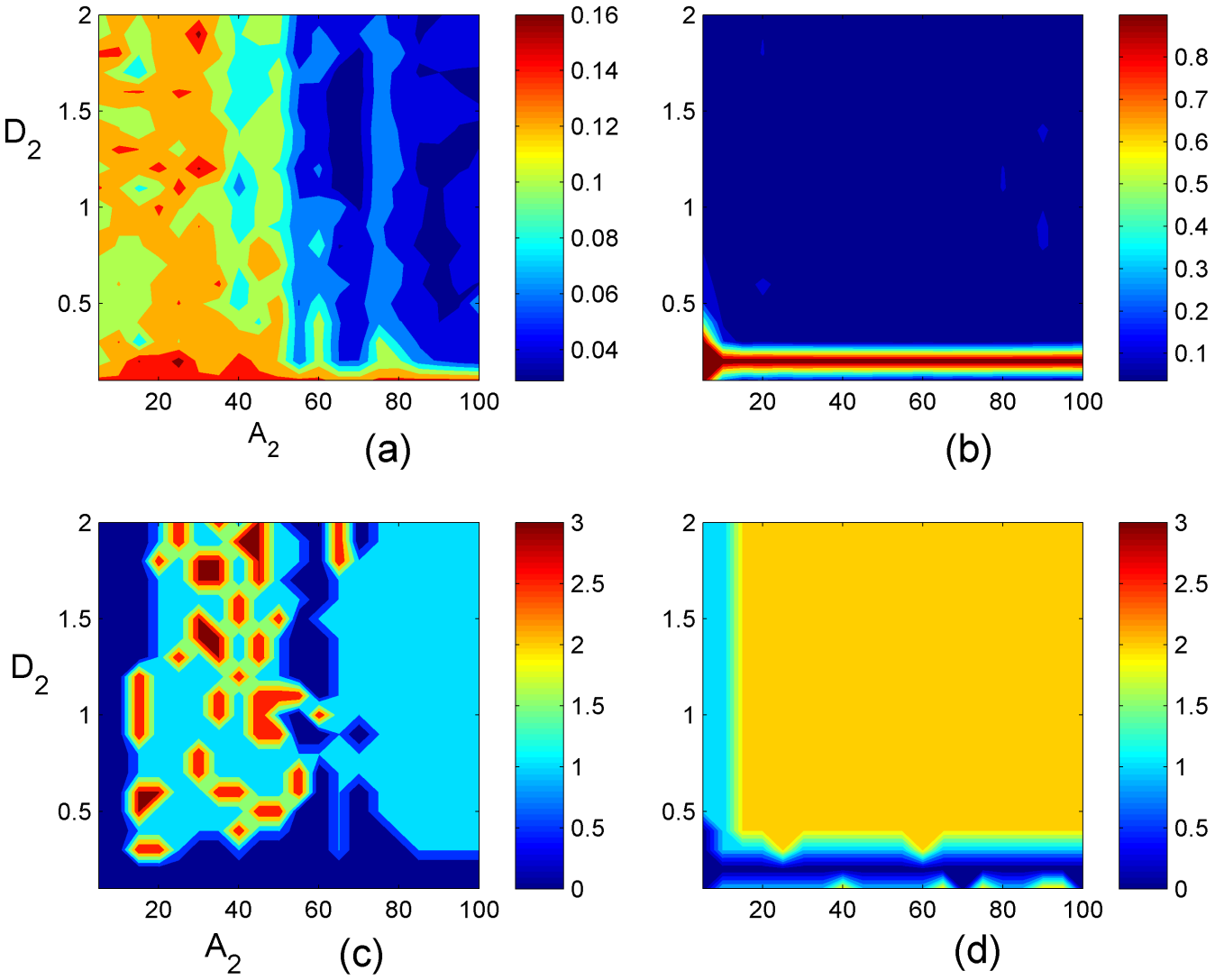

Fig 15. Distribution of factor of synchronization. (a) $D_1 = 0.1$, the distribution of factor of synchronization R in the two-parameter space A_2 and D_2; **(b)** $D_1 = 0.2$ the distribution of factor of synchronization R in the two-parameter space A_2 and D_2; **(c)** $D_1 = 0.1$, the distribution of different patterns in the two-parameter space A_2 and D_2; **(d)** $D_1 = 0.2$, the distribution of different patterns in the two-parameter space A_2 and D_2. (unstable pattern for 0-navy blue; target wave for 1-sky blue; broken patterns for 2-yellow; spiral wave for 3-red).

doi:10.1371/journal.pone.0154282.g015

stability function for the Eq 8 could be written

$$\delta\dot{w} = (DF - \varepsilon DH)\delta w \tag{9}$$

$$DF = \begin{pmatrix} -\alpha 2\pi ab\cos(2\pi bx_0) & \alpha & 0 \\ 1 & -1 & 1 \\ 0 & -\beta & 0 \end{pmatrix} \tag{10}$$

where DF and DH are the Jacobian matrices of functions F and H respectively, and $\varepsilon = k\lambda_k$, λ_k is the eigenvalue of the Laplacian matrix, x_0 is the equilibrium point, and $x_0 = n/(2b)$. As reported in Ref [52], the stability of the synchronization of the system could be affected by the multi-variables coupling. For simplicity, we will analyze the stability of synchronization of the

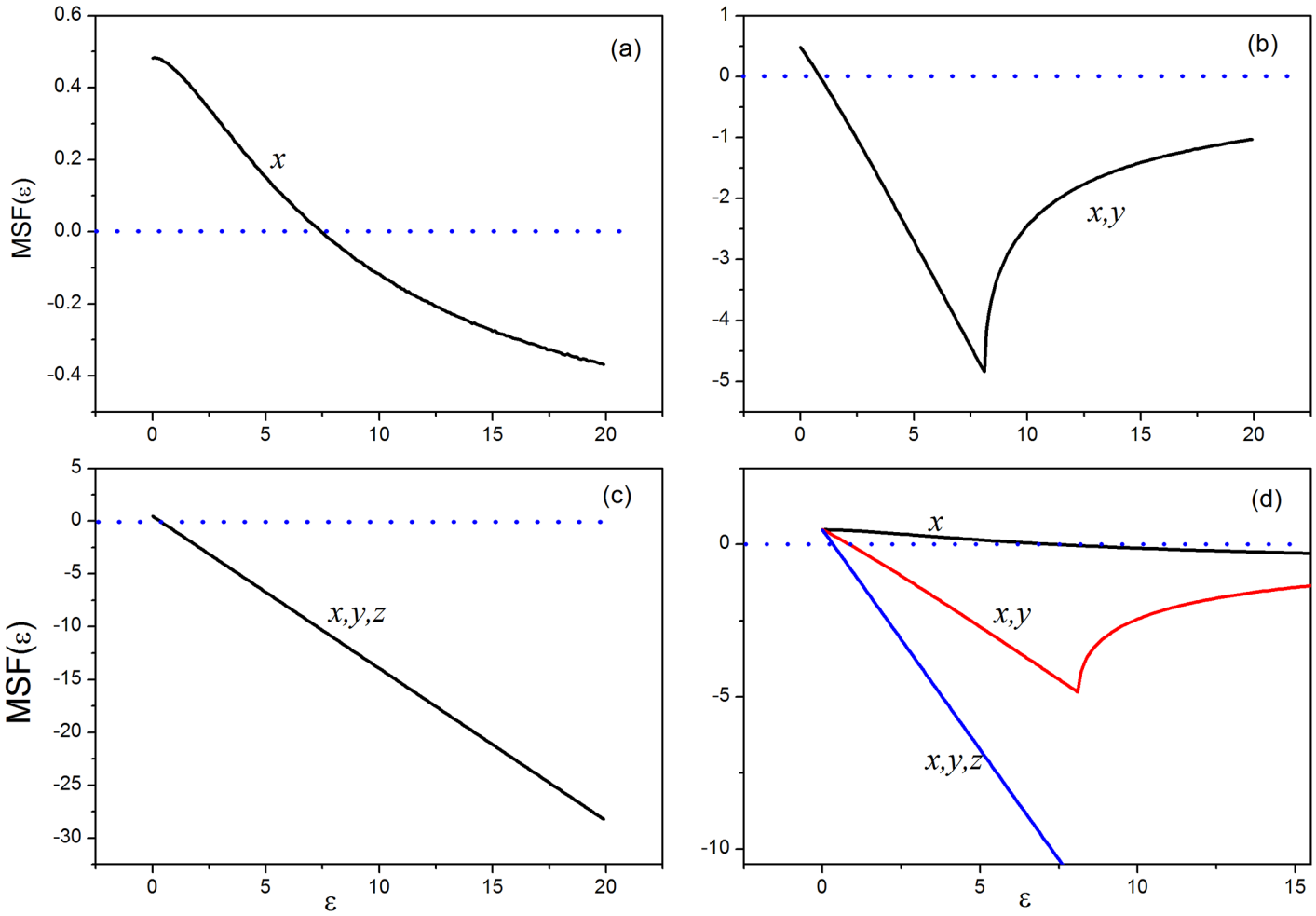

Fig 16. The master stability function MSF(ε) as a function of parameter ε. (a) *x* variable couple, **(b)** two variables coupling (*x*,*y*), **(c)**three variables coupling(*x*,*y*,*z*), **(d)** the results for three kinds of cases are plotted in one figure.

doi:10.1371/journal.pone.0154282.g016

system with only one, two or three variables coupling by Master stability function, respectively. Here the Jacobian matrices for coupling function $H(\boldsymbol{w})$ with different numbers of variables coupling is described by.

$$DH_x = \varepsilon \begin{pmatrix} 1 & 0 & 0 \\ 0 & 0 & 0 \\ 0 & 0 & 0 \end{pmatrix}; DH_{x,y} = \varepsilon \begin{pmatrix} 1 & 0 & 0 \\ 0 & 1 & 0 \\ 0 & 0 & 0 \end{pmatrix}; DH_{x,y,z} = \varepsilon \begin{pmatrix} 1 & 0 & 0 \\ 0 & 1 & 0 \\ 0 & 0 & 1 \end{pmatrix} \quad (11)$$

where DH_x, $DH_{x,y}$, $DH_{x,y,z}$ is the Jacobian matrix for *x* variable, two variables(*x*,*y*) and there variables coupling(*x*,*y*,*z*), respectively. The maximum Lyapunov exponents of Eq 9 as a function of ε are calculated with the three kinds of coupling, respectively. The results are shown in Fig 16.

The results in Fig 16 indicate that the synchronization stability is enhanced with increasing the coupling channels or variables. The stability of synchronizability of the system under three-variables coupling is better than case for two-variables coupling, and two-variables coupling is better than single-variable coupling. Therefore, the synchronizability of the system could be enhanced by multi-variables coupling. As a result, we mainly discussed the pattern selection

and control when nodes are coupled under three-channels. Indeed, the coupling between nodes imposed possible feedback on each node, and it is interesting to the stability of node or circuit under negative feedback.

The analysis of isolated system with negative feedback

The isolated system under negative feedback is described by

$$\begin{cases} \dot{x} = \alpha(y - a\sin(2\pi bx)) - D_1 x \\ \dot{y} = x - y + z - D_2 y \\ \dot{z} = -\beta y - D_3 z \end{cases} \quad (12)$$

where the feedback gains are selected by $D_1 = D_2 = D_3 = D$. Three-channel feedback is considered that three variables (x,y,z) are feedbacked into the isolate circuit, the attractors of the controlled system and bifurcation diagram with different feedback gains are calculated under random initial values in Fig 17.

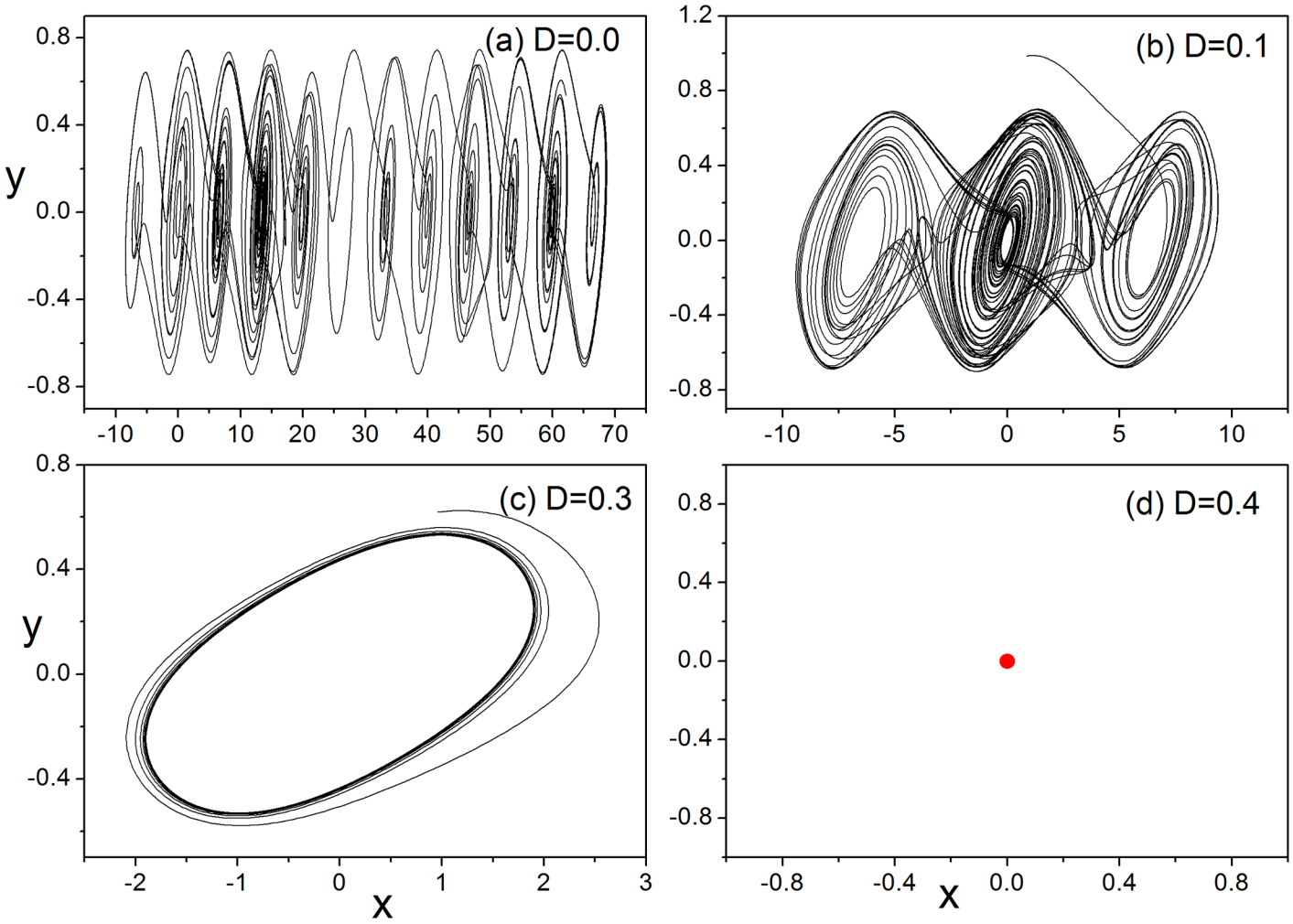

Fig 17. The attractors of the system with different feedback gains. For (a)$D = 0.0$, (b)$D = 0.1$, (c)$D = 0.3$, (d)$D = 0.4$.

doi:10.1371/journal.pone.0154282.g017

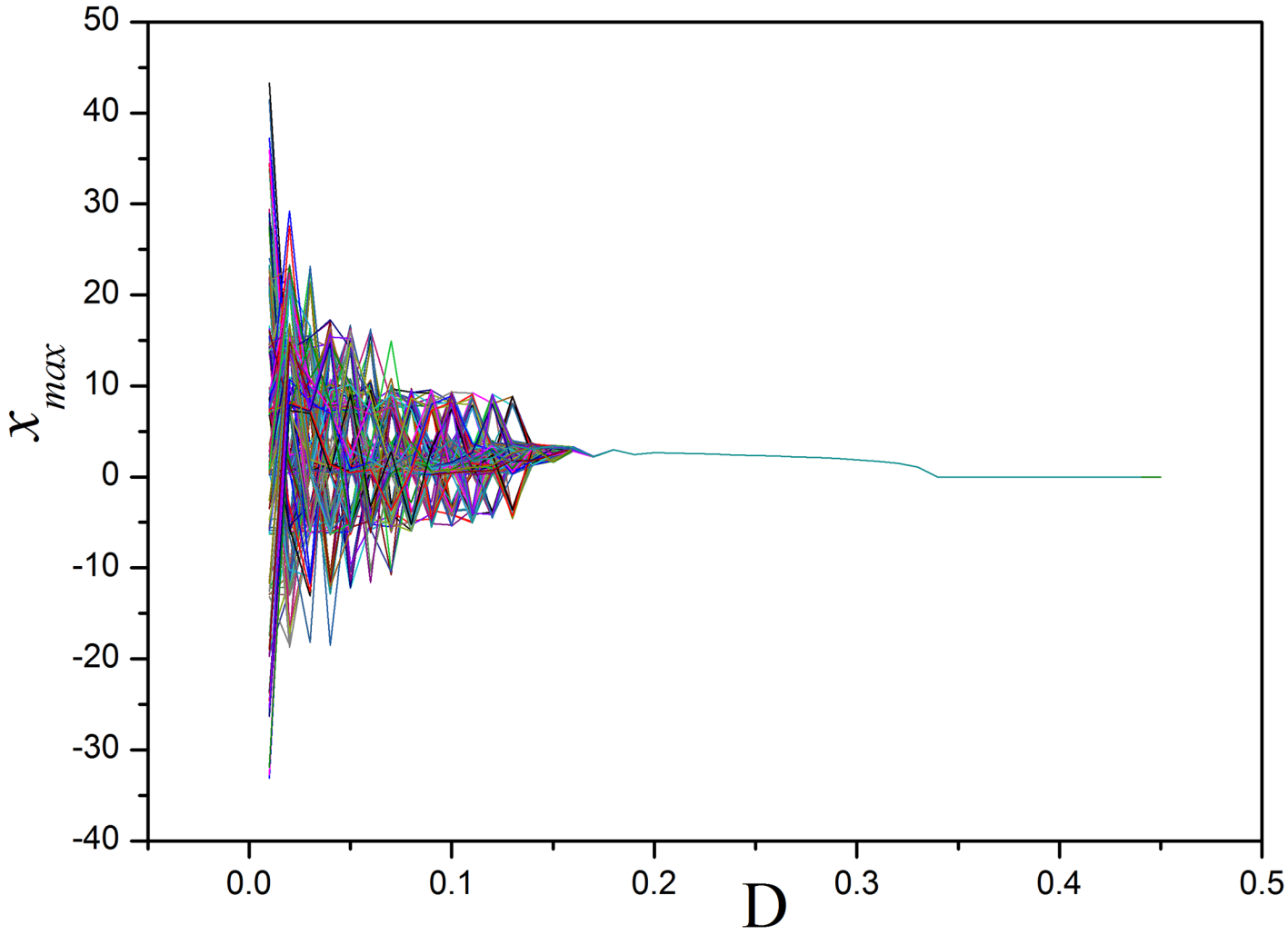

Fig 18. Bifurcation diagram. The bifurcation diagram for the system as a function of feedback gains *D* with three variables (*x*,*y*,*z*) feedback, the random initial values are chosen in the simulation.

doi:10.1371/journal.pone.0154282.g018

The results in Fig 17 confirmed that three-channel feedback on the chaotic circuit makes the system decrease the number of attractors and it even can be stabilized completely. It is also found that multi-channel or multi-variable feedback can control and stabilize the chaotic system effectively than the case for single-channel (or single-variable feedback) and the threshold for feedback intensity can be decreased. Furthermore, the bifurcation diagram for three-channel(or three-variable) feedback is calculated in Fig 18.

The results in Figs 17 and 18 found that the developed state is much dependent on the selection of feedback gain and thus the multi-stability could be adjusted. In a summary, multi-channel or multi-variable feedback, and also multi-channel coupling can be more effective to stabilize the chaotic attractors than single-channel or single-variable feedback or coupling, thus complex spatial patterns could be selected. Therefore, it is also interesting to investigate process of the annihilation of multistability of the system [52,53,54], the basins for an isolated system under different feedback gains are calculated.

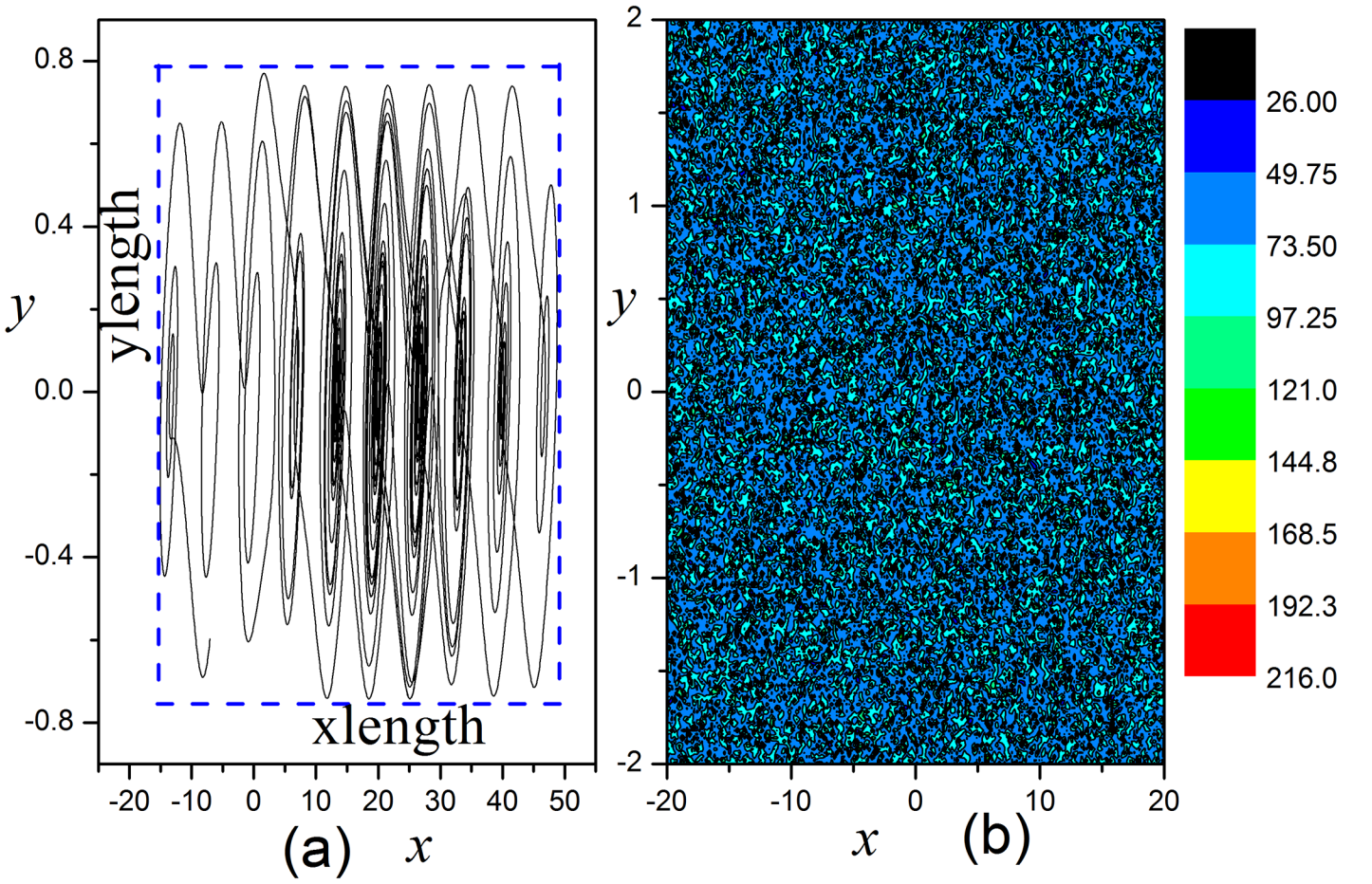

Fig 19. Multi-scroll attractors and basion. (a) The chaotic attractor is developed at t = 300 time units, and D = 0.0. (b) The basin for the system with D = 0.0, initial values of variable x, y are chosen uniformly in the x-y plane box, $x\in[-20,20]$, $y\in[-2,2]$, z = 0.03.

doi:10.1371/journal.pone.0154282.g019

To quantify the state for the system at every node in the basin, the region for the multi-scroll attractor in plane (x, y) is calculated, the scroll area is defined by

$$Area\ size = xlength \times ylength \tag{13}$$

where $xlength = x_{max}-x_{min}$, $ylength = y_{max}-y_{min}$, $x_{max}(y_{max})$ and $x_{min}(y_{min})$ stand for the maximum and minimum value of the variable $x(y)$, respectively. The results in Fig 9(a) show the attractor for the system within 300 time units, and Area size is associated with the scroll number and also the state of the system. During the calculating area size, time series for output variables are used from t = 200 to 300 time units. Different initial values are chosen uniformly in the x-y plane box $x\in[-20,20]$, $y\in[-2,2]$, z = 0.03. The basin for the system with no feedback is calculated in Fig 19(b).

The distribution of basin in Fig 19 confirmed that the developed states are much dependent on the selection of initial values. Furthermore, it is interesting to investigate the transition of basin and states by applying appropriate feedback gains, and the results are plotted in Fig 20.

The results in Fig 20 show that the multistability is gradually annihilated with increasing feedback gains D. In the case of network, the collective behaviors are dependent on the dynamics of each node which can be changed by setting appropriate feedback gain (or coupling intensity). The switch of basin area can induce phase transition of spatial pattern thus

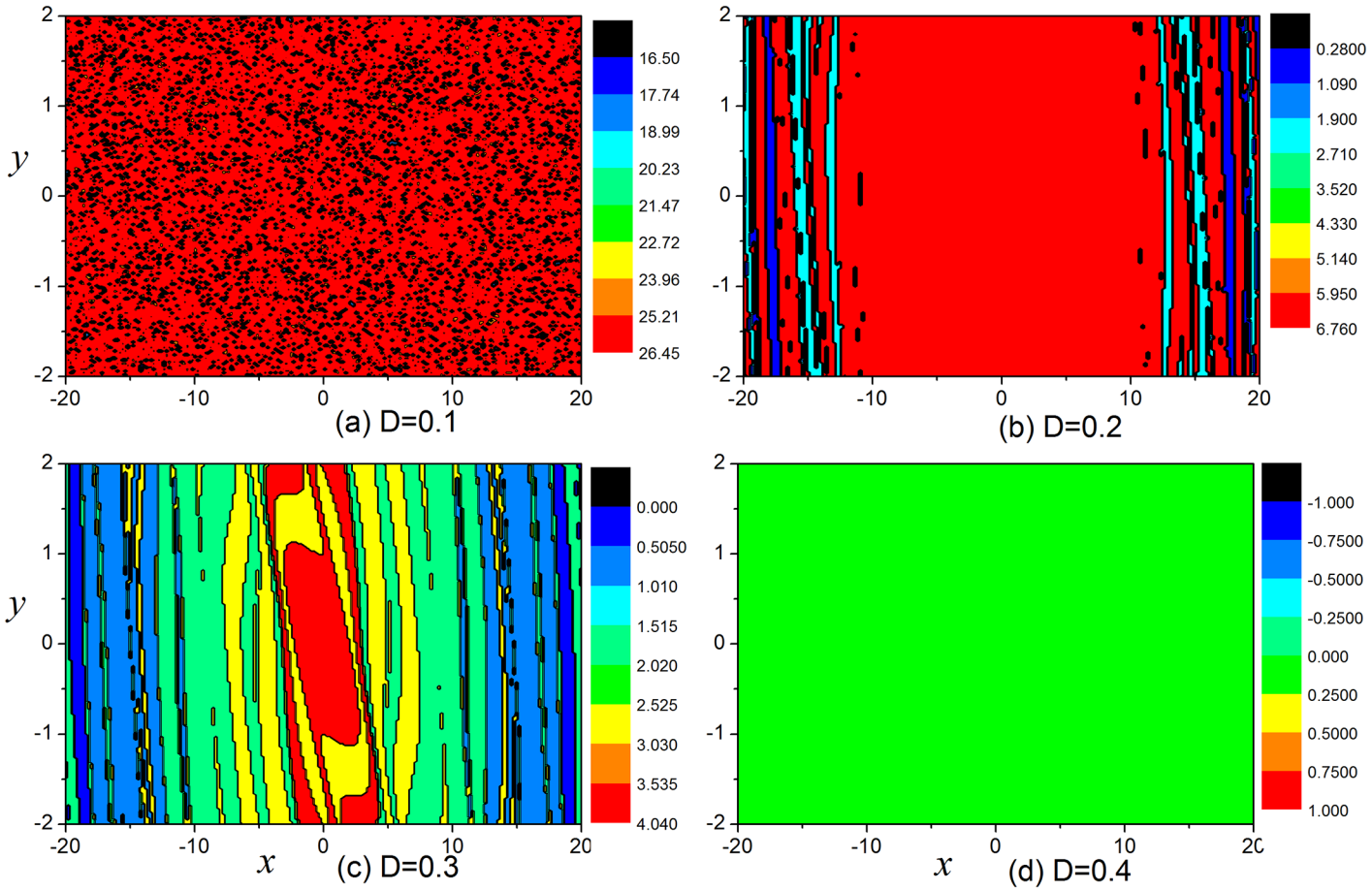

Fig 20. The basin for the system with different feedback gains *D*. For (a) $D = 0.1$, (b) $D = 0.2$, (c) $D = 0.3$, (d) $D = 0.4$, the variables x and y are selected uniformly in the box [–20,20] and [–2,2].

doi:10.1371/journal.pone.0154282.g020

different patterns could be formed in the network under appropriate initial values and coupling intensity.

Conclusions

In this paper, network of coupled multi-scroll attractors is designed to investigate the stability of spatial patterns. It is found that stable spatial pattern can't be formed in regular connection type. By applying negative feedback with diversity, spiral wave, target wave and homogeneous states could be observed in the network. It indicates that spatial patterns could be stabilized and selected under appropriate feedback gain in diversity and controlled area, the factor of synchronization is calculated to discern the effect of diversity in feedback gain and controlled area. It could present a new challengeable problem and useful guidance for network of multi-scroll attractors.

Supporting Information

S1 File. Supporting data for Fig 20a at D = 0.1.
(DAT)

S2 File. Supporting data for Fig 20b at D = 0.2.
(DAT)

S3 File. Supporting data for Fig 20c at D = 0.3.
(DAT)

S4 File. Supporting data for Fig 20d at D = 0.3.
(DAT)

Author Contributions

Conceived and designed the experiments: JM FL. Performed the experiments: FL. Analyzed the data: JM FL. Contributed reagents/materials/analysis tools: FL. Wrote the paper: JM FL.

References

1. Gray R A, Pertsov A M, Jalife J (1998) Spatial and temporal organization during cardiac fibrillation. Nature (London) 392:75–78
2. Bär M, Gottschalk N, Eiswirth M, Ertl G (1994) Spiral waves in a surface reaction: model calculations. J Chem Phys 100:1202
3. Gray R A, Jalife J, Panfilov A V, Baxter W T(1995) Mechanisms of cardiac fibrillation. Science 270:1222 PMID: 7502055
4. Holden A V(1997) The restless heart of a spiral, Nature 387(6634): 655–666
5. Atarashi H(1999) Historical perspectives on the mechanism of atrial fibrillation. J Cardiol Suppl 33: 53
6. Fenton F H, Cherry E M, Hastings H M, Evans S J(2002) Multiple mechanisms of spiral wave breakup in a model of cardiac electrical activity. Chaos 12:852–892 PMID: 12779613
7. Xu Y, Jin WY, Ma J (2015) Emergence and robustness of target waves in a neuronal network. Int J Mod Phys B 29:1550164
8. Jiang M X, Wang X N, Ouyang Q, Zhang H (2004) Spatiotemporal chaos control with a target wave in the complex Ginzburg-Landau equation system. Phys Rev E 69: 056202
9. Xiao J H, Hu G, Zhang H, Hu B B(2005) Controlling the breakup of spiral waves in an excitable medium by applying time-delay feedback signals. Europhys Lett 69:29–35
10. Shajahan T K, Nayak A R, Pandit R(2009) Spiral-Wave Turbulence and Its Control in the Presence of Inhomogeneities in Four Mathematical Models of Cardiac Tissue. PLoS ONE 4: e4738 doi: 10.1371/journal.pone.0004738 PMID: 19270753
11. Cross M C, Hohenberg P C(1993) Pattern formation outside of equilibrium. Rev Mod Phys 65: 851–1112
12. Yagisita H, Mimura M, Yamada M(1998) Spiral wave behaviors in an excitable reaction-diffusion system on a sphere. Physica D 124:126–136
13. Gollub J P, Langer J S(1999) Pattern formation in nonequilibrium physics. Rev Mod Phys 71: 396–403
14. Roth B J(2001) Meandering of spiral waves in anisotropic cardiac tissue. Physica D 150: 127–136
15. Goryachev A, Kapral R(1996) Spiral waves in chaotic systems, Phys Rev Lett 76:1619 PMID: 10060475
16. Li W B, Zhang H,Ying H P, Hu G(2009) Coherent wave patterns sustained by a localized inhomogeneity in an excitable medium. Phys Rev E 79:026220
17. He D H, Hu G, Zhan M(2002) Pattern formation of spiral waves in an inhomogeneous medium with small-world connections. Phys Rev E 65: 055204
18. Wu X Y, Ma J(2013) The Formation Mechanism of Defects, Spiral Wave in the Network of Neurons. PLoS One 8: e554031
19. Perc M(2007) Effects of small-world connectivity on noise-induced temporal and spatial order in neural media. Chaos, Solitons and Fractals 31:280–291
20. Ma J, Wu Y, Wu N J, Guo H Y (2013)Detection of ordered wave in the networks of neurons with changeable connection, Sci China Phys Mech Astron 56: 952–959
21. Qin H X, Ma J, Wang C N, Chu R T(2014) Autapse-induced target wave, spiral wave in regular network of neurons, Sci China Phys Mech Astron 57:1918–1926

22. Roxin A, Riecke H, Solla S A(2004) Self-sustained activity in a small-world network of excitable neurons. Phys Rev Lett 92: 98101
23. Wang Q Y, Perc M, Duan Z S, Chen G R(2008) Delay-enhanced coherence of spiral waves in noisy Hodgkin-Huxley neuronal networks. Phys Lett A 372:5681–5687
24. Erichsen R, Brunnet LG(2008) Multistability in networks of Hindmarsh-Rose neurons. Phys Rev E 78: 061917
25. Huang X Y, Troy W C, Yang Q, Ma H T, Laing C R, Schiff S J et al.(2004) Spiral waves in disinhibited mammalian cortex. J Neurosci 24: 9897 PMID: 15525774
26. Schiff S J, Huang X Y, Wu J Y(2007) Dynamical evolution of spatiotemporal patterns in mammalian middle cortex, Phys Rev Lett 98: 178102 PMID: 17501537
27. Huang X Y, Xu W F, Liang J M, Takagaki K, Gao X, Wu J Y(2010) Spiral Wave Dynamics in Neocortex. Neuron 68:978–990 doi: 10.1016/j.neuron.2010.11.007 PMID: 21145009
28. Ma J, Liu Q R, Ying H P, Wu Y(2013), Emergence of spiral wave induced by defects block. Commun Nonlinear Sci Numer Simulat 18:1665–1675
29. Ma J, Wang C N, Ying H P, Wu Y, Chu R T(2013) Emergence of target waves in neuronal networks due to diverse forcing currents. Sci China Phys Mech Astron 56: 1126–1138.
30. Stich M, Mikhailov A S(2006) Target patterns in two-dimensional heterogeneous oscillatory reaction—diffusion systems. Physica D 215:38–45
31. Gosak M, Marhl M, Perc M(2009) Pacemaker-guided noise-induced spatial periodicity in excitable media. Physica D 238:506–515
32. Hou Z H, Xin H W(2002) Noise-Sustained Spiral Waves: Effect of Spatial and Temporal Memory. Phys Rev Lett 89:280601 PMID: 12513128
33. Tang Z, Li Y Y, Xi L, Jia B, Gu H G(2012) Spiral waves and multiple spatial coherence resonances induced by the colored noise in neuronal network. Commun Theor Phys 57: 61–67
34. Gu H G, Jia B, Li Y Y, Chen G R(2013) White noise-induced spiral waves and multiple spatial coherence resonances in a neuronal network with type I excitability. Physica A 392:1361–1374
35. Luo J M, Zhan M(2008) Electric-field-induced wave groupings of spiral waves with oscillatory dispersion relation. Phys Rev E 78:016214
36. Cai M C, Pan J T, Zhang H(2012) Electric-field-sustained spiral waves in subexcitable media. Phys Rev E 86: 016208
37. Chen J X, Hu B B(2008) Spiral breakup and consequent patterns induced by strong polarized advective field. EPL 84:34002
38. Jiang L L, Zhou T, Perc M, Huang X, Wang B H(2009) Emergence of target waves in paced populations of cyclically competing species. New J Phys 11:103001
39. Ma J, Tang J(2015) A review for dynamics of collective behaviors of network of neurons. Sci China Tech Sci 58:2038–2045
40. Wang Q Y, Zheng Y H, Ma J(2013) Cooperative dynamics in neuronal networks. Chaos Solitions and Fractals 56:19–27
41. Yalcin M E, Suykens J A K, Vandewalle J (2002) Families of scroll grid attractors. Int J Bifurcat Chaos 12(1): 23–41
42. Lü J H, Chen G R, Yu X H, Leung H(2004) Design and analysis of multi-scroll chaotic attractors from saturated function series. IEEE Trans Circ Syst 51(12): 2476–2490
43. Demirkol A S, Ozoguz S, Tavas V, Kilinç S(2008) A CMOS realization of a double-scroll chaotic circuit and its application to random bit number generation. IEEE Proc ISCAS 2374–2377
44. Suykens A K, Vandewalle J(1993) Generation of *n*-Double Scrolls. IEEE Trans Circ Syst I 40: 861–867
45. Yalçin M E (2007) Multi-scroll and hypercube attractors from a general jerk circuit using Josephson junctions. Chaos, Solitons and Fractals 34:1659–1666
46. Tang W K S, Zhong G Q, Chen G R, Man K F(2001) Generation of N-scroll attractors via Sine function. IEEE Trans Circ Syst I 48:1369–1372
47. Ma J, Wu X Y, Chu R T, Zhang L P(2013) Selection of multi-scroll attractors in Jerk circuits and their verification using Pspice. Nonlinear Dyn 76:1951–1962.
48. Li F, Yao C G (2016) The infinite-scrolls attractor and energy transition in chaotic circuit. Nonlinear Dyn doi: 10.1007/s11071-016-2646-z
49. Gonze D, Bernard S, Waltermann C, Kramer A, Herzel H (2005) Spontaneous synchronization of coupled circadian oscillators. Biophys J 89:120–129. PMID: 15849258

50. Heagy J F, Carroll T L, Pecora L M (1994) Synchronous chaos in coupled system. Phys Rev E 50: 1974–1885

51. Pecora L M, Carroll T L, (1998) Master stability functions for synchronized coupled systems. Phys Rev Lett 80:2109–2111

52. Sevilla-Escoboza R, Gutiérrez R, Huerta-Cuellar G, Boccaletti S, Gómez-Gardeñes J, Arenas A et al. (2015) Enhancing the stability of the synchronization of multivariable coupled oscillators. Phys Rev E 92:032804

53. Pisarchik A N, Feudel U (2014) Control of multistability. Phys Rep 540:167–218

54. Sevilla-Escoboza R, Pisarchik A N, Jaimes-Reátegui R, Huerta-Cuellar G (2015) Selective monostability in multi-stable systems. Proc R Soc A 471:20150005